

**AN AC–DC HYBRID NANOGRID SYSTEM
WITH SWITCHED CAPACITOR INTERLEAVED
BIDIRECTIONAL CONVERTER**

A PROJECT REPORT

submitted by

AMINA SHAJAHAN

TKM21EEPS02

to

the APJ Abdul Kalam Technological University

in partial fulfillment of the requirements for the award of the

Degree

of

Master of Technology

in

Power Systems



**DEPARTMENT OF ELECTRICAL AND ELECTRONICS
ENGINEERING**

T.K.M. COLLEGE OF ENGINEERING, KOLLAM

APRIL-MAY, 2023

DEPARTMENT OF ELECTRICAL AND ELECTRONICS
ENGINEERING.

T.K.M COLLEGE OF ENGINEERING, KOLLAM



CERTIFICATE

This is to certify that the report entitled '**An AC–DC Hybrid Nanogrid System with Switched Capacitor Interleaved Bidirectional Converter**' submitted by **Amina Shajahan** to the APJ Abdul Kalam Technological University in partial fulfillment of the requirements for the award of the Degree of Master of Technology in Electrical and Electronics Engineering is a bonafide record of the project work work carried out by her under our guidance and supervision. This project report in any form has not been submitted to any other University or Institute for any purpose.

Prof. Baiju R Naina

(External Examiner)

Internal Supervisor

Associate Professor

Dept of EEE, TKMCE

Prof. Jibi P Mathew

Dr. Sabeena Beevi K

Project Coordinator

Head of Department

Asst. Professor

Professor

Dept of EEE, TKMCE

Dept of EEE, TKMCE

ACKNOWLEDGEMENT

First of all I am indebted to the **God Almighty** for giving me an opportunity to excel in my effort to complete this project on time.

I am extremely grateful to **Dr. T. Shahul Hameed**, Principal, TKM College of Engineering, and **Dr. Sabeena Beevi. K**, Head of the Department, Department of Electrical and Electronics Engineering, for providing all required resources for successful completion of my project.

I am greatly obliged to **Prof. Shanavas T. N.**, Associate Professor, PG co-ordinator, Department of Electrical and Electronics Engineering, for his encouragement and support.

My heartfelt gratitude to **Prof. Baiju R Naina** , Associate Professor, Project Guide, Department of Electrical and Electronics Engineering, for her valuable suggestions and guidance in the preparation of the project report.

I express my thanks to **Prof. Jibi P Mathew** , Asst. Professor, Project co-ordinator, Department of Electrical and Electronics Engineering, and all staff members and friends for all help and co-ordination extended in bringing out this project successfully in time.

I will be failing in duty if I do not acknowledge with grateful thanks to the authors of the references and other literature referred to in this project.

Last but not at the least, I am very much thankful to my parents who guided me in every steps which I took.

Place: Kollam

Date: April-May 2023

AMINA SHAJAHAN

TKM21EEPS02

ABSTRACT

A hybrid AC-DC nanogrid system with PV and battery storage is designed, to fulfill most of the nanogrid's energy requirement from renewable energy source (RES) installed in the building itself i.e., from solar energy. Of late, most of the modern loads like LED based lighting loads, digital computer, television, mobile phone chargers, BLDC Fans, electric vehicle charger, modern refrigerators and air conditioning units require DC for its function. In a conventional system the DC from the RES converts to AC and then converts back to DC with a series of unnecessary conversion stages. The number of conversion stages can be reduced by directly providing multiple levels of DC buses (for low voltage loads, HV loads & Medium Voltages loads) along with conventional AC bus (230 V, 50 Hz) for the AC loads (Heating loads, AC motors etc.). This process will improve the reliability of the system significantly. This system requires a bidirectional DC-DC converter for the designing of DC Buses. Initially the system is designed using cascaded buck boost bidirectional converter and is then modified with switched capacitor interleaved bidirectional converter to reduce ripples, voltage stress and to improve the efficiency.

Contents

Acknowledgement	i
Abstract	ii
Contents	v
List of Figures	viii
List of Tables	ix
Abbreviations	x
1 Introduction	1
1.1 General Background	1
1.2 Motivation	4
1.3 Thesis objectives	4
1.4 Structure of thesis	5
1.4.1 Chapter 1	5
1.4.2 Chapter 2	5
1.4.3 Chapter 3	6
1.4.4 Chapter 4	6
1.4.5 Chapter 5	6
2 Literature Survey	7
2.1 Introduction	7

2.2	An AC–DC Hybrid Nanogrid System for PV and Battery Storage Based Futuristic Buildings	7
2.3	Variable Load Demand Scheme for Hybrid AC/DC Nanogrid	8
2.4	A Comparative Study on Voltage Level Standard for DC Residential Power Systems	9
2.5	DC distribution for residential power networks; A framework to analyze the impact of voltage levels on energy efficiency	10
2.6	AC vs. DC Home: An Efficiency Comparison	11
2.7	A Novel Single-Stage Single-Phase Reconfigurable Inverter Topology for a Solar Powered Hybrid AC/DC Home	12
2.8	DC, Come home: DC microgrids and the birth of the “Enernet”	14
2.9	Simulation Analysis of Grid-connected AC/DC Hybrid Microgrid	16
2.10	Operation and Control of a Hybrid AC–DC Nanogrid for Future Community Houses	18
2.11	Power Management for a Hybrid AC/DC Microgrid With Multiple Subgrids	20
2.12	Conclusion	21
3	Methodology	23
3.1	Introduction	23
3.2	Research on existing systems	24
3.3	Proposed system	24
3.4	Design of PV MPPT Boost Converter	25
3.4.1	PV Array Sizing	25
3.4.2	MPPT Control design	26
3.4.3	Design of Boost Converter	28
3.5	Design of Bidirectional Buck boost converter to battery & Cascaded bidirectional converter	28
3.5.1	Design of Bidirectional Buck boost Converter	28
3.6	Design of Grid connected H bridge inverter	29
3.7	Switched Capacitor Interleaved Bidirectional Converter	30

3.7.1	Modes of operation	31
3.7.2	Design	31
3.8	Proposed system modification	32
3.9	Conclusion	33
4	Simulation	34
4.1	Introduction	34
4.2	PV MPPT Boost Converter	34
4.2.1	MPPT Control	35
4.3	Bidirectional buck boost converter	36
4.4	Cascaded Bidirectional buck boost converter	37
4.5	Grid connected single phase H bridge Square wave Inverter	38
4.6	Grid connected single phase H bridge sine wave Inverter	39
4.7	Switched capacitor interleaved bidirectional converter	41
4.8	Conclusion	43
5	Results and Discussions	44
5.1	Introduction	44
5.2	Results with Cascaded buck boost bidirectional converter	44
5.3	Results with Switched capacitor interleaved bidirectional converter	50
5.4	Conclusion	53
6	Conclusion	54
	Publications	55
	References	56

List of Figures

1.1	Photovoltaic Potential- India	2
1.2	Solar Installation Trends in India	3
1.3	Conventional and modern building	4
2.1	An AC-DC hybrid Nanogrid system	8
2.2	New microgrid power distribution topologies in buildings.	10
2.3	Proposed configuration of a DC home microgrid.	12
2.4	New microgrid power distribution topologies in buildings.	14
2.5	Configuration of grid-connected hybrid AC/DC microgrid.	17
2.6	Primary and secondary control levels of the considered NG system.	19
2.7	Topology of the hybrid ac/dc microgrid.	21
3.1	Methodology	23
3.2	Proposed System	24
3.3	PV Characteristics	26
3.4	Flowchart of Incremental Conductance	27
3.5	SCIB Converter configuration	30
3.6	Double loop control diagram. (a) Step-up mode (b) Step-down mode	30
3.7	Current-flow paths in the step-up mode	31
3.8	Current-flow paths in the step-down mode	31
3.9	Proposed System modification	32
4.1	PV MPPT Boost Converter	35
4.2	Incremental Conductance algorithm	35

4.3	Battery bus with bidirectional buck boost converter and its control	36
4.4	Battery bus with cascaded bidirectional buck boost converter	37
4.5	Cascaded bidirectional buck boost converter control	37
4.6	Grid connected single phase H bridge square wave Inverter with its control	38
4.7	Grid connected single phase H bridge sine wave Inverter	39
4.8	H bridge sine wave Inverter control	40
4.9	Switched capacitor interleaved bidirectional converter	41
4.10	Open loop control of SCIB converter in buck mode	42
4.11	Open loop control of SCIB converter in boost mode	42
4.12	Closed loop control of SCIB converter in buck mode	43
4.13	Closed loop control of SCIB converter in boost mode	43
5.1	DC Bus Voltages	45
5.2	DC Bus Currents	45
5.3	Voltage across switches S1,S2	46
5.4	Voltage across switches S3,S4	46
5.5	AC grid Voltage	47
5.6	H bridge Square wave Inverter output Voltage	47
5.7	Synchronised AC grid voltage and inverter voltage with square wave inverter	48
5.8	Synchronised AC grid current and inverter current with square wave inverter	48
5.9	Synchronised AC grid voltage and inverter voltage with sine wave inverter	49
5.10	THD Analysis of AC sine wave inverter output	49
5.11	DC Bus voltages	50
5.12	DC Bus Currents	50
5.13	Voltage across switches Q1-Q4	51
5.14	Voltage across switches Q5-Q8	51
5.15	Synchronised AC grid voltage and inverter voltage	52

5.16 THD Analysis of AC sine wave inverter output	52
---	----

List of Tables

3.1 Panel generation factor 25

5.1 Comparison of Converter output quality 53

Abbreviations and Notations

1. RES: Renewable Energy Sources
2. PV : Photovoltaic
3. MPPT : Maximum Power Point Tracking
4. PLL : Phase Locked Loop
5. SCIB : Switched Capacitor Interleaved Bidirectional
6. BDC : Bidirectional DC-DC Converter

Chapter 1

Introduction

1.1 General Background

More than a century ago, an electric grid was created to transport energy from generating units to end users. This is one of the biggest physical network in the world and every country in the world use this network in different dimensions. According to predictions, the world's total energy usage will reach 37,000 terawatt hours by 2030 on account of the population growth. Cities require power in the tune of two-thirds of the world's overall demand. Distribution losses on long-distance transmission lines are rising, which lowers grid effectiveness. As nearly 31 billion tonnes of CO_2 are generated each year, which has a grave impact on global warming, the cost of electricity for fossil fuel-based power plants is rising daily. Due to an inefficient utility infrastructure, the nearly 1.2 billion people in remote regions still live without access to electricity.

In future, most of the buildings will rely more on locally available renewable energy sources for their energy needs. Solar electricity is one of the RES that gains popularity due to its sustainability. India has a huge potential for harnessing solar energy. With roughly 300 days of clear, sunny weather each year, India's land region receives an estimated 5 quadrillion kilowatt-hours (kWh) of solar energy.

The amount of solar energy produced in a single year is greater than the total amount of fossil fuel energy sources in India combined. Therefore, India’s solar power business is expanding quickly. As of 28 February 2023, the nation had 64.381 GWAC of total solar power India’s use of solar energy will place fourth worldwide in 2021. In 2018, in India rooftop solar electricity accounted for 2.1 GW[12].

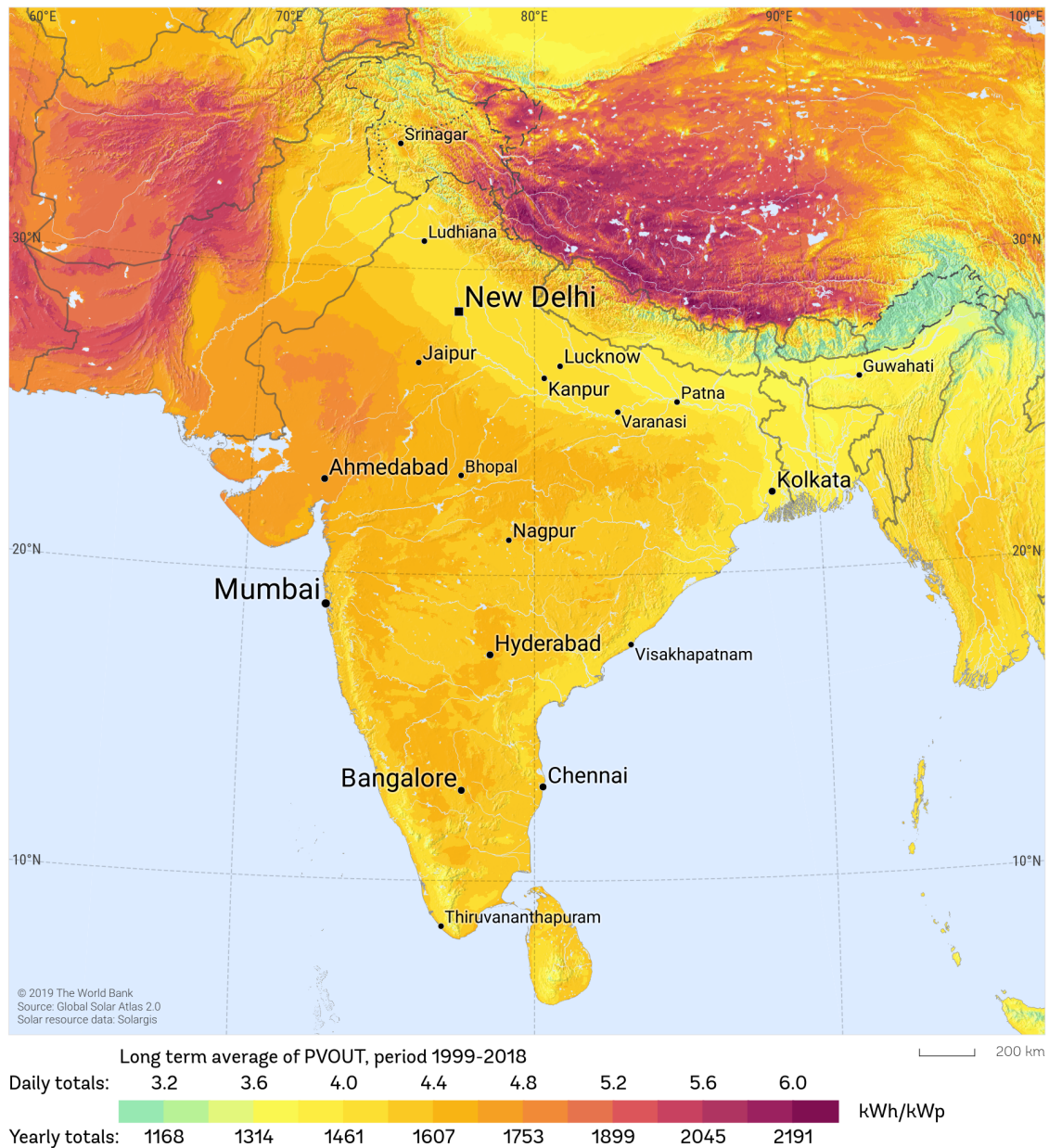


Fig. 1.1: Photovoltaic Potential- India

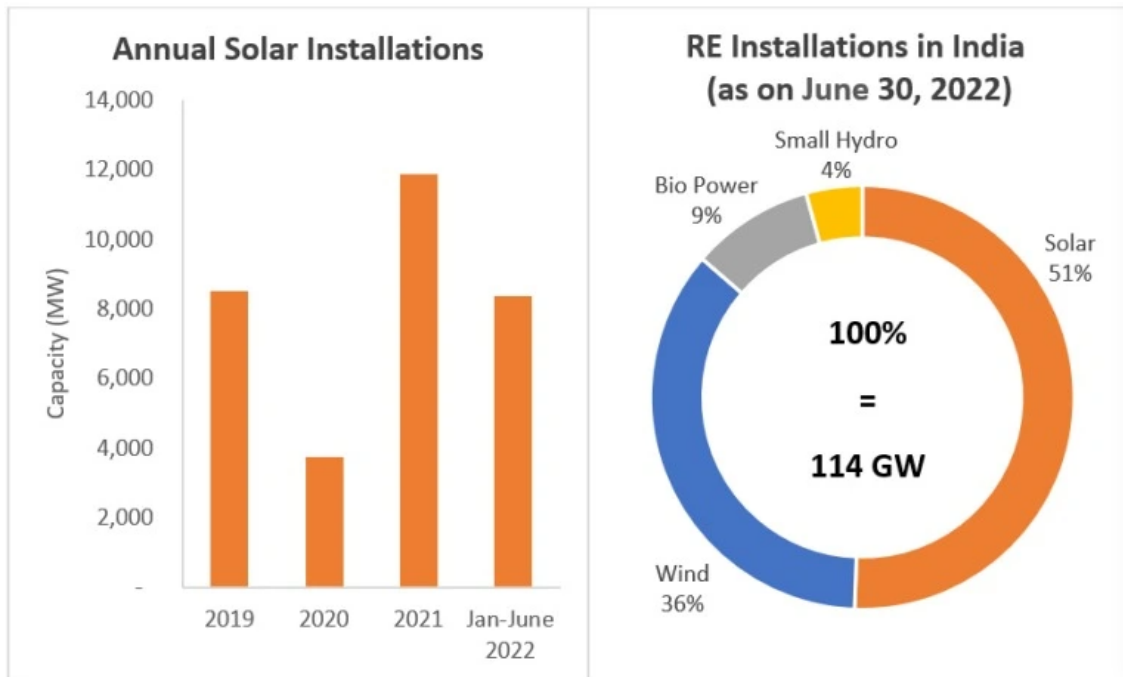


Fig. 1.2: Solar Installation Trends in India

In addition, the majority of modern loads, including digital computers, televisions, mobile phone chargers, LED and CFL-based lighting loads, etc., are dc in character. Also, they require low voltage (LV) dc supply for their operation. Therefore, they are typically interfaced to a 48-V dc bus in order for the PV, aforesaid dc loads, and battery to operate at their best. Depending on their voltage requirements, modern inverter controlled variable speed compressor based refrigerators, air conditioners, and washing machines can be interfaced to a dc bus. Furthermore, there are certain heating loads for which 230-V ac or 230-V dc is typically preferred. It should be noted that the number of conversion stages can be reduced if the loads and RES, which are basically dc in nature, are connected to the proper dc buses rather than the typical ac bus (230 V, 50 Hz or 110 V, 60 Hz). This enhances the system's general reliability and compactness. Additionally, this lowers the ac grid current's total harmonic content. However, ceiling fans, conventional fluorescent lamps, and the loads must all be connected to the traditional ac grid in some residential structures with conventional single-phase induction motor-based pumping loads.

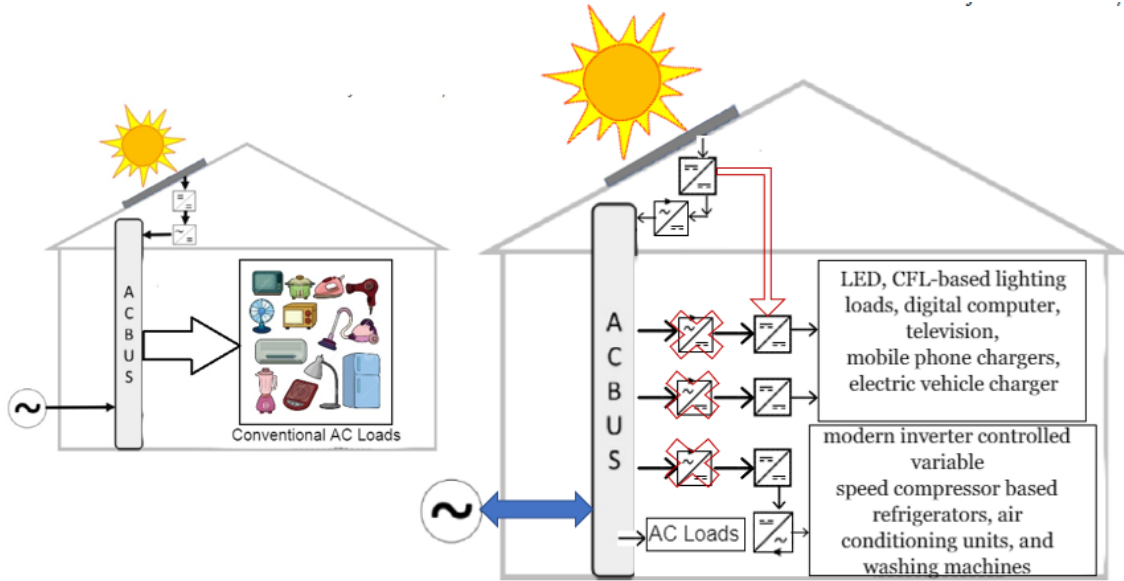


Fig. 1.3: Conventional and modern building

1.2 Motivation

The idea of DC distribution is not novel; it has been used extensively in communication networks, traction systems, and ships. The prevalence of DC household appliances, particularly those with variable-speed motors, LED and CFL lighting loads, digital computers, televisions, and chargers for electric vehicles and mobile phones, among other things, has made this issue more important today. Another significant factor influencing the growth of building DC distribution is the growing use of distributed renewable DC sources, such as photovoltaics (PV). DC energy generated locally must first be converted into AC, and possibly back again for DC appliances, if only AC distribution is used. Major drawbacks of this multi-stage conversion include the requirement for power converters, higher losses, and decreased power reliability. Therefore, the introduction of an AC-DC hybrid nanogrid system is the final answer to this issue.

1.3 Thesis objectives

Based on extensive literature studies, it has been determined that the 100-year-old legacy grid is incompatible with modern DC-based loads, and that a hybrid

AC-DC nanogrid is required given the growing integration of rooftop solar. The major objectives identified are:

- To design a PV battery storage based AC-DC hybrid nanogrid system with four different DC voltage buses and an AC bus for supplying AC loads and grid using cascaded buck boost bidirectional converter.
- Open loop simulation of switched capacitor interleaved bidirectional converter
- Closed loop simulation of switched capacitor interleaved bidirectional converter
- To design a PV battery storage based AC-DC hybrid nanogrid system with four different DC voltage buses and an AC bus for supplying AC loads and grid using switched capacitor interleaved bidirectional converter
- Study and compare the performance of the system with cascaded buck boost bidirectional converter and SCIB Converter.
- Achieve reduced ripples & voltage stress and to improve the efficiency & voltage gain in output.

1.4 Structure of thesis

1.4.1 Chapter 1

This chapter emphasises the present issues the traditional grid is facing as well as the development of modern DC-based loads and the growing integration of PV. It deals with the problem of unnecessary DC to AC conversion stages and related losses. The motivation, objective and structure of the thesis are also covered in this part.

1.4.2 Chapter 2

This chapter discusses the various literatures referred as a part of this project.

A comprehensive description of these works are provided in this chapter.

1.4.3 Chapter 3

The modelling of the entire system is covered in Chapter 3. It describes the sizing of the PV system as well as the design of various components of boost, bidirectional converter, inverter, etc. This chapter also explains the different phases of the project's execution as well as how the proposed and modified system operate.

1.4.4 Chapter 4

This chapter deals with the simulation of various components like PV, Boost, Bidirectional converter, Inverter etc. The simulations of both proposed and modified system are also explained in this chapter.

1.4.5 Chapter 5

The exhaustive simulation studies depicting the proposed system along with the modified system have been carried out, and the results are presented in this chapter. The result discussion and comparisons are also described at the chapter ending.

Chapter 2

Literature Survey

2.1 Introduction

This chapter provides an overview of the topics that supplied the ideas for this project. The following sections examine the previous works which have been done on the similar topics.

2.2 An AC–DC Hybrid Nanogrid System for PV and Battery Storage Based Futuristic Buildings

In this paper, a seven-bus ac-dc hybrid nanogrid system for future buildings and its associated control strategy are suggested. One ac bus and six dc buses can run simultaneously on the nanogrid, and power from any bus can be seamlessly transferred to any other bus. The ac bus, two DC buses, and stand-alone mode operation are all features of their respective designs. The other two DC lines are used to connect the battery storage to solar photovoltaic (PV) systems. The two dc buses that remain are set up to handle loads at medium voltage levels. The ability of some of the buses to be reconfigured expands the range of household appliances

that can be powered by the nanogrid. The low voltage rating of the battery bus and the PV bus, respectively, is intended to reduce the series connection of batteries and PV modules. Additionally, the PV array's need for fewer series-connected modules reduces the impact of shading, which is typically a problem with roof-top installations. In addition, the system is created transformer-free, which reduces its size, volume, and weight in comparison to plans that use line frequency transformers.

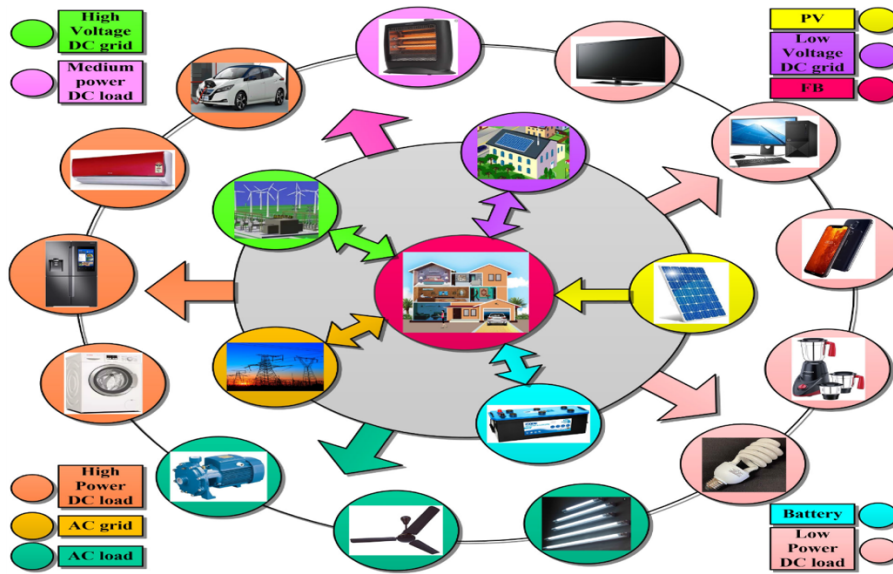


Fig. 2.1: An AC-DC hybrid Nanogrid system

2.3 Variable Load Demand Scheme for Hybrid AC/DC Nanogrid

The use of nanogrid technology to handle the problem of widespread load shedding for domestic consumers is the topic of this paper. To achieve this, various load control strategies, load classification, and maximising solar energy are used. This study is novel because it includes DC-based load in the basic load, DC inverter load in the regular load, and schedules the burst load for when solar PV generation is at its highest. In numerous publications to date, the word "nanogrid" as a power structure has remained ambiguous. The goal of this article was to provide a clear

definition of nanogrid. One of the key components of the nanogrid is demand side load management, which allows end users to understand key aspects of their peak energy usage and off peak hours. A microgrid option with a facility for the nanogrid leads to a system that is more reliable with improvements in efficiency and a drop in carbon emissions. When DC power from PV plants is used directly, the loss is automatically reduced to 16%. The AC/DC combination nanogrid is 63% more efficient than an AC-only system. Compared to a nanogrid that uses only DC, this one has efficiency gains of almost 18%. The demand curve is smoothed by 54% more during intelligent load shifting than it is during traditional load shifting. Real-time pricing is more cost-effective than flat rate tariff for a home without DG, but flat rate results are more cost-effective when DG are used in nanogrids, according to simulation findings. If only flat prices are used for DG in nanogrid instead of real-time pricing, savings of 12.67% - 21.46% are made.

2.4 A Comparative Study on Voltage Level Standard for DC Residential Power Systems

Recent years have seen an increase in interest in the application and study of residential low voltage DC (LVDC) power systems due to the rising demand for the integration of renewable energy sources and DC power usage. The residential DC power system has benefits in the integration of distributed generation and the reduction of conversion costs, which could offer customers a high-efficiency and high-quality power supply. However, the industrial application of the LVDC power system is hindered by the absence of voltage level standards. In order to offer DC power suppliers and appliance manufacturers voltage level recommendations, a thorough study of the effectiveness of various voltage levels is suggested in this paper.

Current voltage choices are compared to one another in terms of power source, topology, power supply capability, electrical safety and voltage compatibility from applications and study. The residential DC power system model of a neighbourhood with four residential subsystems is used to perform comparative simulation. Based

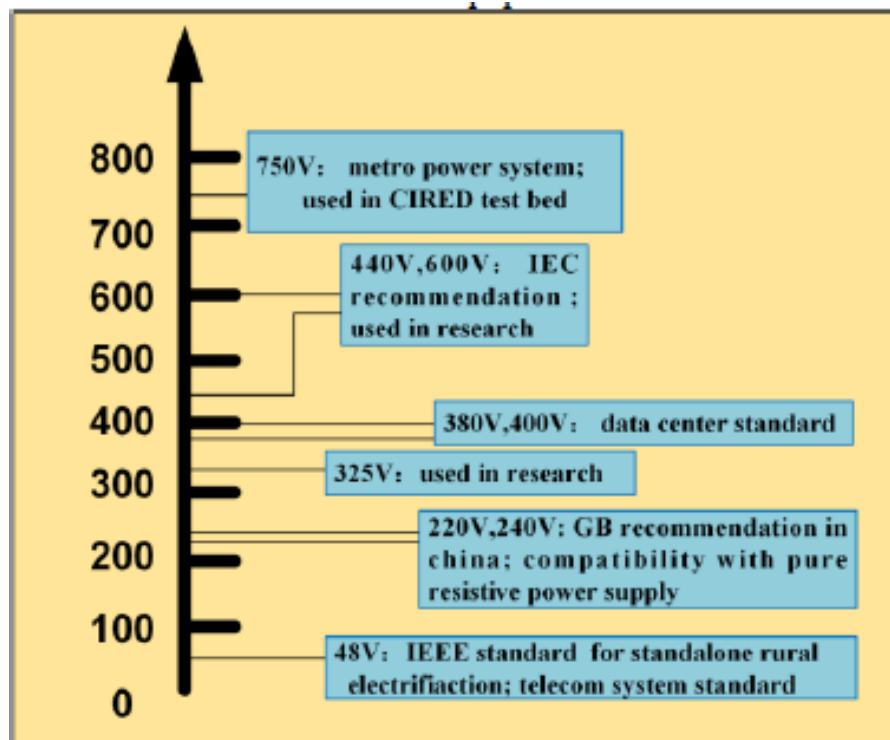


Fig. 2.2: New microgrid power distribution topologies in buildings.

on the simulation and investigation, the comparison outcome shows that: 375V bipolar DC system should be used in heavy load conditions; 240V and 380V is optimal for unipolar domestic systems with low power consumption.

2.5 DC distribution for residential power networks; A framework to analyze the impact of voltage levels on energy efficiency

Residential DC networks have grown in popularity in recent years, largely as a result of photovoltaic systems incorporated into buildings, rising electronic loads, and dropping prices for DC appliances. The current standards for DC distribution, which range from 48V to 380V and impact system efficiency, are fragmented in comparison to AC (110V, 60Hz, or 220V, 50Hz). In this study, we develop a framework to evaluate the effect of different voltages on distribution losses and power electronic conversion losses in residential systems. The system efficiency for a typ-

ical DC home is then assessed at 48 V, 220 V, and 380 V DC and compared with 220 V AC using the established analytical framework and simulation. According to the findings, the DC system at 220 V and 380 V is 4% and 10% more efficient than the AC 220 V system, respectively, for a medium-sized solar integrated home. Additionally, for cable sizes AWG-6 and larger, the system efficiency for 48 V DC is greater than 380 V DC. Even though the efficiency relies on a number of variables, including conductor size, voltage choice, connected loads, and solar capacity, the framework provided is essential for quantifying losses and choosing the right system components for a DC home.

2.6 AC vs. DC Home: An Efficiency Comparison

The starting of electric transmission saw the battle between AC and DC as power transfer medium. As it lacked the capacity for voltage transformation at that point, DC lost the dispute. However, as power electronics technology advanced, Power Electronic Converters (PECs) were created and developed, which led to the revival of DC. A further argument in favour of DC is that the tendency is moving towards DC loads and that the majority of modern energy-efficient appliances are DC-operated. By contrasting the efficiency of AC and DC homes, this paper offers insight into the distribution scale energy savings possibilities of DC.

Two distinct topologies—one with a main PEC supplying all the loads and the other with separate PEC for each load; creating a total of four configurations, are taken into consideration when analysing the AC and DC home's efficiency values. Systems are simulated for various PEC efficiencies while taking daily load fluctuation into account. The findings show that DC systems outperform AC systems in terms of efficiency, with advantages of 3.62 and 3.88 percent for bulk and separate PEC topologies, respectively.

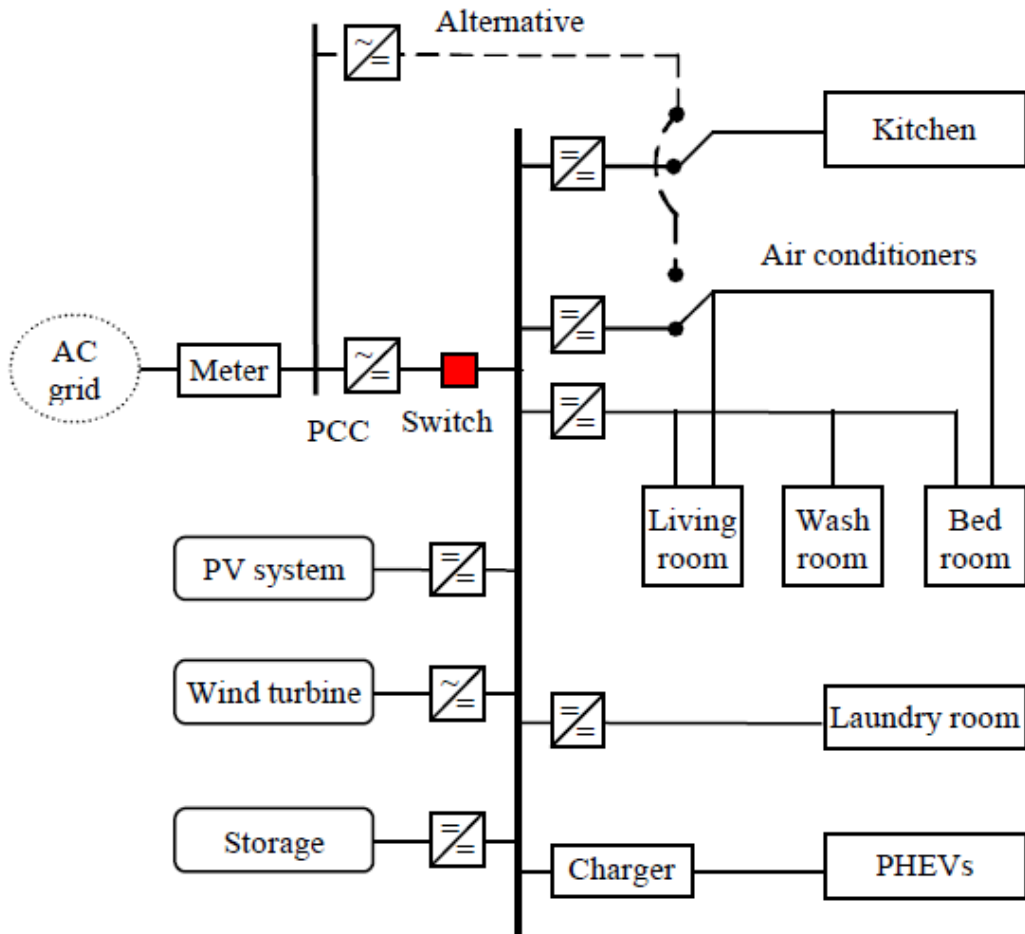


Fig. 2.3: Proposed configuration of a DC home microgrid.

2.7 A Novel Single-Stage Single-Phase Reconfigurable Inverter Topology for a Solar Powered Hybrid AC/DC Home

For a hybrid ac/dc solar-powered home, this paper proposes a reconfigurable single-phase inverter topology. The primary benefit of this converter is that it can operate in dc/dc, dc/ac, and grid tie modes, which lowers loss, cost, and converter size. This converter has a single-phase single-stage topology. Appliances in this hybrid ac/dc house are powered by both currents. This style of house improves the harmonic profile by isolating dc loads to the dc supply side and the remainder to the ac side, which reduces power loss by avoiding unnecessary double stages of

power conversion. The simulation is carried out in MATLAB/Simulink, and the hardware implementation using an Arduino Uno controller is used to verify the findings. Such a solar-powered home with this innovative inverter topology could serve as a fundamental building component for an energy-efficient smart grid and microgrid in the future.

The main objective of this paper is the implementation of a single-phase single-stage solar converter known as a reconfigurable solar converter (RSC) in a residential building that is powered by solar energy and has energy storage systems. The fundamental idea behind the RSC is to use a single power conversion system to perform various operational modes for solar PV systems with energy storage, including solar PV to grid (Inverter operation, dc-ac), solar PV to battery/dc loads (Dc-Dc operation), battery to grid (Dc-ac), battery/PV to grid (Dc-ac), and Grid to battery (Ac-Dc). A hybrid ac/dc home powered by solar energy is used to evaluate this inverter, which has both ac and dc domestic loads. The harmonic contributions that specific appliances make to the distribution grid from a typical contemporary home are taken into account when choosing which ones to use. In addition to the aforementioned, there have also been the following accomplishments. Sensors and electrical components vary, and a typical inductor is only used for dc/dc operation. Solar PV-battery functioning is confirmed while taking solar radiation variation into account. The switches operating in the architecture for dc/dc operation reduce the circulation current. In this paper, control logic and input quantity sampling vary as well.

This study recommended an improved converter topology for a hybrid ac/dc home fueled by solar energy. Using a single conversion of ac power to dc and vice versa is the primary concept behind this topology, which increases efficiency, decreases volume, and improves reliability. The converter topologies proposed are helpful in reducing a significant amount of harmonics in the residential feeders of the future smart grid, according to the hardware implementation. Although only solar PV is used here as a power source, this design could also be used with wind, fuel cells, etc.

2.8 DC, Come home: DC microgrids and the birth of the “Enernet”

Making power industry history is the topic of this paper. It is about the possibility for dc power, the first type of electrical power, to once more change the world. With the aid of contemporary solid-state power electronics technology, it is revived. Buildings that “cleanly” produce enough energy on-site to equal the energy they consume, producing a “net zero” balance at the building level, are referred to as ZEBs, at least in the context of this article. This further opens up the possibility of reducing the total negative effects of energy production on our economy, climate, and environment. From these and other related initiatives globally, a number of common approaches to designing for low- or zero-energy buildings, whether they are new or existing, are emerging.

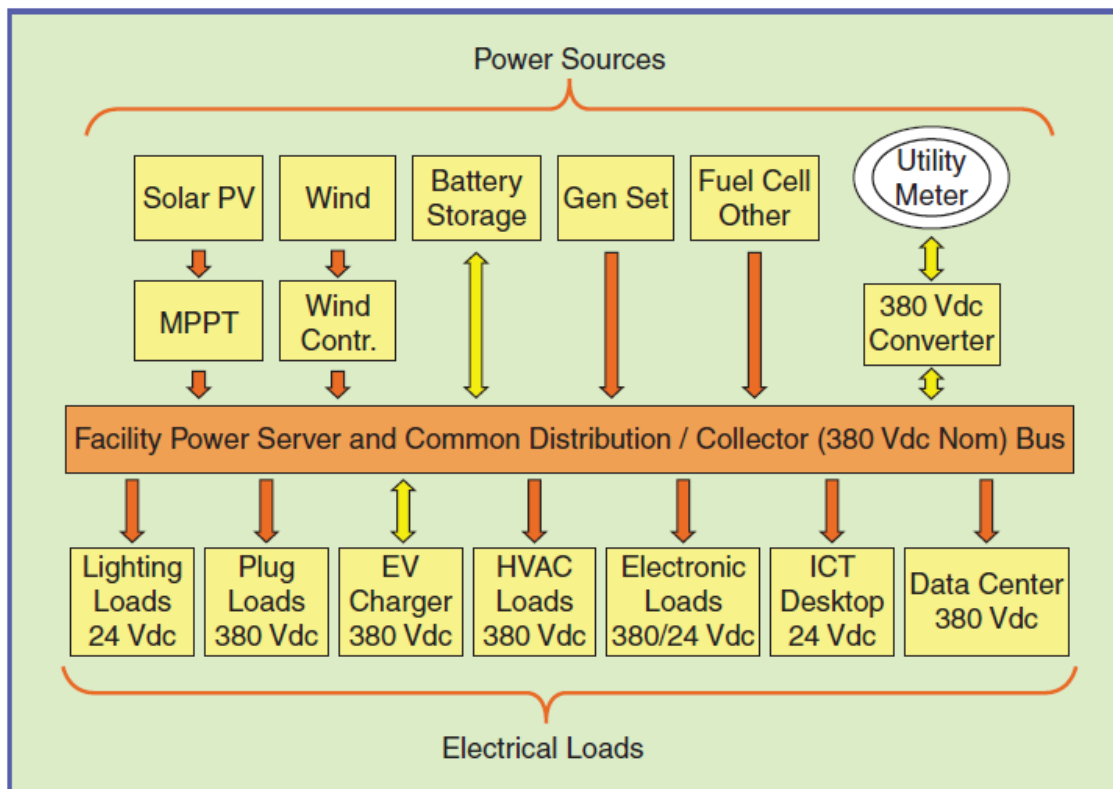


Fig. 2.4: New microgrid power distribution topologies in buildings.

Lighting is frequently a top priority, both in terms of boosting day lighting

and improving the energy efficiency of the remaining electric light. In addition, a variety of new design approaches are being used in mechanical and heating, ventilation, and air-conditioning (HVAC) systems. These include updated ventilation plans, the application of cutting-edge technologies like chilled beams and radiant panels, as well as increased use of variable-speed drive motors for pumps and air handlers. Controls and building technology are added by so-called "smart building" methodologies. On-site power generation and storage, which includes the use of solar, wind, and other renewable energy generation, as well as more effective power distribution throughout a building, are other areas of emphasis. Design strategies are evolving generally for new construction and extensive renovation projects, with an increasing emphasis on the 2030 challenge.

The key areas of application in buildings for standardization of dc power use include:

- the need for dc electricity is primarily driven by lighting and control loads in interiors and occupied areas
- Data centres and telecom central offices, along with the ICT (information and communications technology) equipment use dc.
- electric car charging and outdoor light-emitting diode (LED) lighting are two examples of outdoor electrical applications of DC
- Utilities, building services and HVAC with electronic dc motorised machinery and variable-speed drives (VSD).
- differences in power protection device and safety application
- building-level electrification cannot use dc due to a lack of robust environment.
- An uncertain transition from dc-inclusive distribution methods to ac-centric distribution models.

2.9 Simulation Analysis of Grid-connected AC/DC Hybrid Microgrid

This article proposes an AC/DC hybrid microgrid with loads, energy storages, and some renewable energy sources (PV, fuel cell). Both ac and dc microgrids make up the hybrid microgrid. The power flow between the ac microgrid and the dc microgrid is controlled by a bi-directional AC/DC converter. The fuel cell and PV array's dc side via the DC/DC converter attached to the dc bus. Through a bi-directional DC/DC converter, a battery serving as an energy storage device is linked to the DC bus. The DC/DC/AC converter is used to link the PV array on the ac side to the ac bus. The ac microgrid drives the suggested hybrid microgrid's operation in grid-connected mode. The simulation test-bed is then implemented using MATLAB/Simulink after each module's model and control approach have been examined. The steady state of the system, the transient process of switching the fuel cell, the change of solar irradiance on both the ac and dc sides, and the change of the AC and DC loads are used to model the impact of system operation. With the final conclusions, the simulation analysis results for the operation characteristics and transient process of grid-connected operation under various circumstances are given.

A grid-connected AC/DC hybrid microgrid is described in this article. The system model is then constructed in MATLAB/Simulink after each module's model and control strategy have been thoroughly explained. The system's operation features are examined in both the system's steady state and its instantaneous state, which includes the sudden switching of the load between the ac and dc sides, the switching of the fuel cell on the dc side, and the altering of solar irradiance between the ac and dc sides. The Operating characteristics are as follows:

- Energy storage equipment does not participate in power balance in the hybrid AC/DC microgrid in a steady state, where all distributed energy sources run steadily and supply energy to the load. Instead, the utility grid absorbs any excess power.

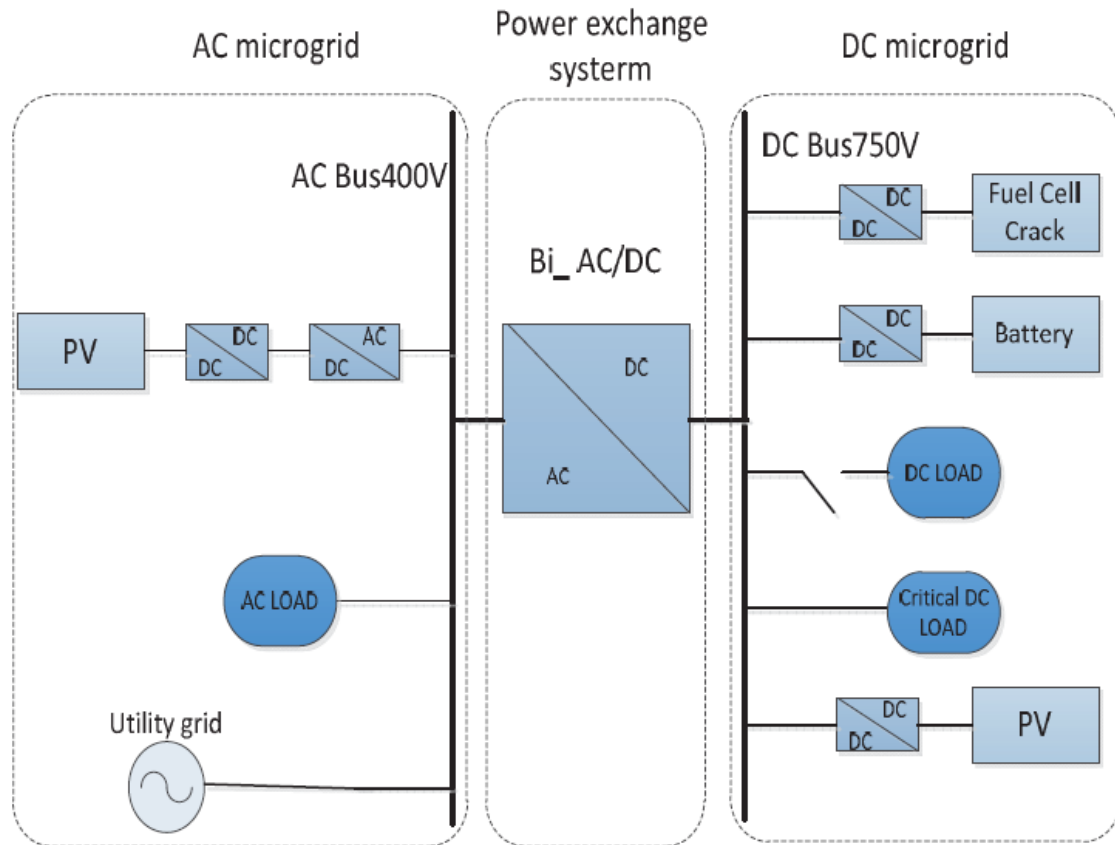


Fig. 2.5: Configuration of grid-connected hybrid AC/DC microgrid.

- The energy storage device is operating at charging or discharging at the switching moment when the dc side load and fuel cell are removed or accessed instantly. However, the dc bus voltage is quickly restored to a new steady state with the assistance of the battery, and the AC microgrid is unaffected by DC microgrid disturbances.
- Ac bus voltage will rise or fall at the switching moment when an ac side load is removed or instantly accessed, but the utility grid will keep the stability of the AC microgrid, and the DC microgrid won't be affected by ac load changes.
- The output power of PV changes as a result of variations in sun irradiance. The battery will discharge in order to keep the stability of the dc bus voltage when the PV and fuel cell power of the DC microgrid are not enough to satisfy the load demand. The lack of power is primarily supplied by the AC microgrid and the bi-directional AC/DC inverter operating in inverter mode. The utility

grid provides the short-cut power to the ac microgrid to keep system stability when the solar irradiance changes on the ac side.

2.10 Operation and Control of a Hybrid AC–DC Nanogrid for Future Community Houses

Future community housing can be thought of as having a hybrid AC-DC nanogrid (NG) power supply infrastructure. This document describes how an NG operates and is controlled. An AC bus and a DC bus are linked by a tie-converter to form the NG. There may be a number of loads and micro sources on each vehicle. The NG should be able to exchange power with the utility system and have sufficient generation capacity to power its loads in off-grid mode. In the event of off-grid operation, the tie-converter switches electricity between two buses and controls bus voltage in both buses. The AC and DC buses are connected using a tie-converter (TC). Additionally, a solid-state static switch and a three-phase transformer are used to supply power to the AC bus, which is also linked to the grid. A few loads and generation devices are linked to each bus. In this research, a 30 kVA, three-phase transformer is used to supply a three-phase, 400 V system for the AC bus and a 350 V DC system for the DC bus. It is speculated that two power-electronic interfaced DERs are connected to the AC bus, and that two additional power-electronic interfaced DERs are connected to the DC bus.

By changing the reference values for the primary controller as needed, the secondary level control (central controller) is in charge of controlling the magnitude and frequency of the voltage in the AC bus as well as the voltage in the DC bus. The central controller takes action based on new rated voltage and frequency references to shift up or down the DERs droop characteristic, if the voltage magnitude or frequency in the AC bus or the voltage magnitude in the DC bus rises above or declines below the acceptable pre-defined values. The central controller's efficacy for various NG operating modes is summed up as follows:

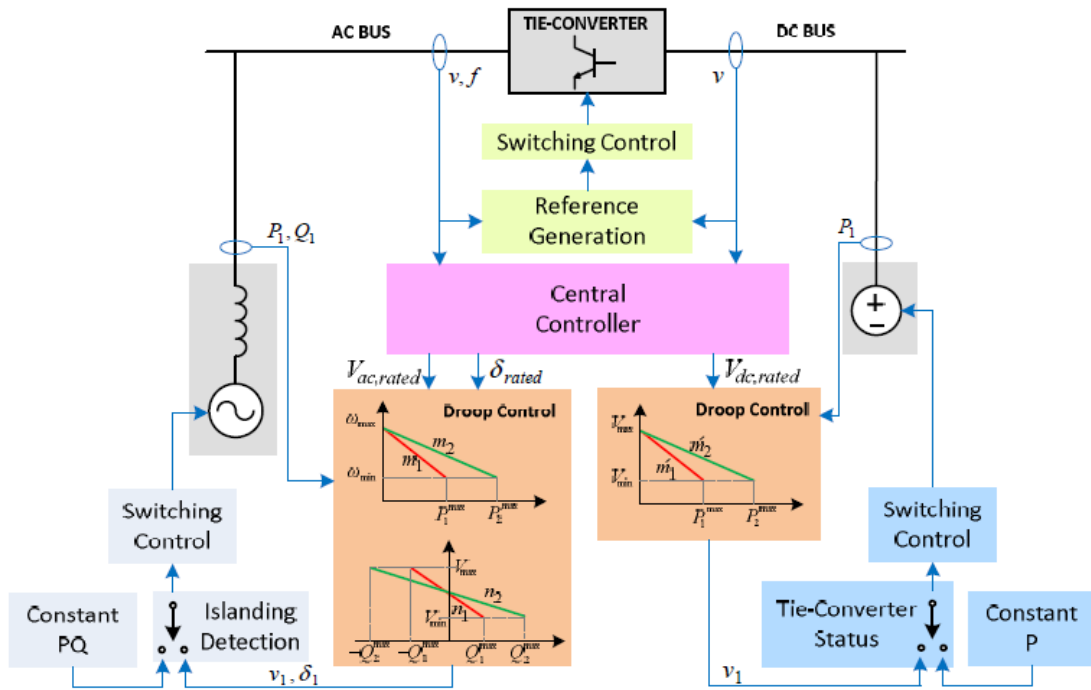


Fig. 2.6: Primary and secondary control levels of the considered NG system.

- The central controller will serve as the secondary level management for each DER in the AC and DC bus if the NG is off-grid. In this scenario, the central controller will specify both the rated voltage for the DERs in the DC bus and the rated voltage magnitude and frequency for the DERs in the AC bus.
- The central controller only has to specify the rated voltage magnitude for the DERs in the DC bus if the AC bus of the NG is connected to the grid while the TC is off because the DERs in the AC bus are capable of exchanging power with the grid and are running in constant PQ mode.
- The central controller is inactive and not controlling the voltage and frequency in the AC or DC bus if the NG's AC bus is attached to the grid while the TC is on.

2.11 Power Management for a Hybrid AC/DC Microgrid With Multiple Subgrids

This study suggests a novel topology for a hybrid ac/dc microgrid in which the system's bidirectional ac/dc converters (BADCs) and bidirectional dc/dc converters (BDDCs) link various subgrids to a common bus. For various applications, the rated ac frequencies in various ac subgrids and the rated dc voltages in various dc subgrids can vary. For simple management and high efficiency, the system's storages are grouped together to create a storage subgrid that keeps the common bus voltage constant. A suitable power management technique is required to regulate the power flow among various subgrids in order to guarantee the hybrid micro-grid functions properly. In order to make the interconnected subgrids operate cohesively and provide support for one another, this article suggests a decentralised power management strategy for hybrid microgrids. First, a Pdc v2 dc droop control strategy is suggested to maintain the common bus voltage and to enable power sharing among storages in the storage subgrid while taking the characteristics of the common bus configuration into account. Second, a coordinated power control strategy based on the common bus voltage, ac subgrid frequency, and dc subgrid voltage is created for the BADCs and BDDCs to realise the power interaction among various subgrids because doing so is more complicated than doing so with a conventional hybrid. The suggested approach also considers the capacities and load types of each subgrid; as a result, it can guarantee the power quality of the subgrids with a high percentage of critical loads even when the capacities of the subgrids are out of balance. Real-time hardware-in-loop tests confirm the suggested power management method's efficacy.

This paper proposes a novel hybrid ac/dc microgrid topology with multiple subgrids and a decentralised power management approach for this kind of hybrid microgrid. The decentralised power management approach that has been suggested can enable the interconnected subgrids to cooperate and assist one another. First, a Pdc-vdc2 droop control strategy is suggested to maintain the common bus voltage

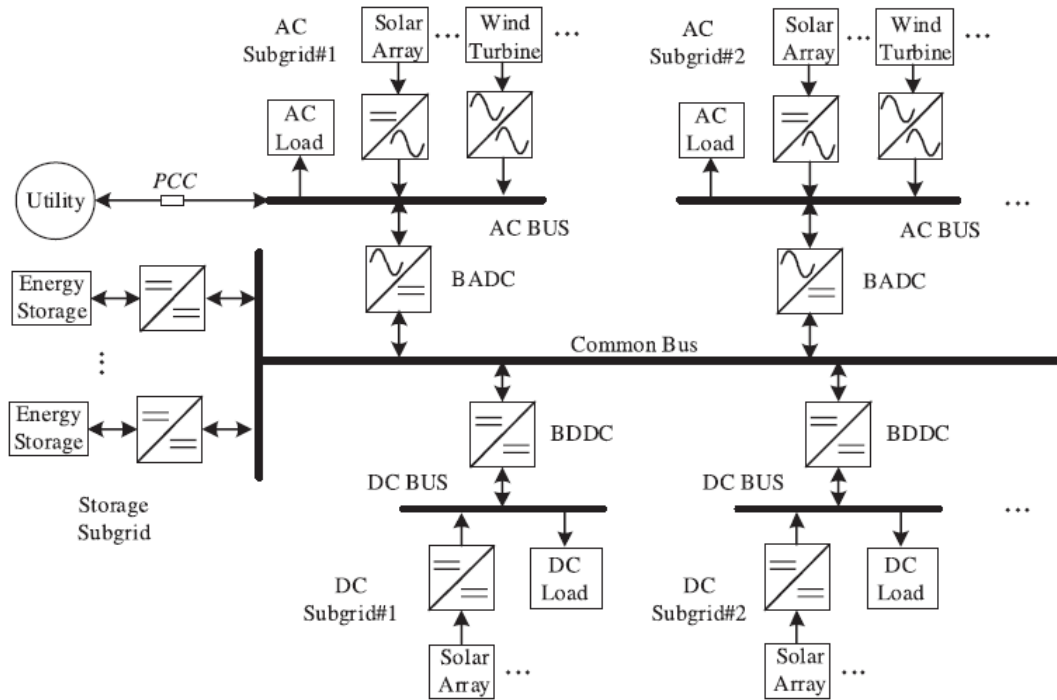


Fig. 2.7: Topology of the hybrid ac/dc microgrid.

and to enable power sharing among storages in the storage subgrid while taking the characteristics of the common bus configuration into account. Second, a coordinated power control strategy based on the common bus voltage, ac subgrid frequency, and dc subgrid voltage is created for the BADCs and BDDCs to realise the power interaction among various subgrids because doing so is more complicated than carrying it out in a conventional hybrid. Additionally, the suggested strategy takes into account the capacities and load types of each subgrid; as a result, it can still be used when the capacities of subgrids are out of sync and can guarantee the power quality of subgrids with a high percentage of crucial loads. Additionally, the related HIL tests are carried out to confirm the efficacy of the suggested power management.

2.12 Conclusion

This section summarises the findings on the detailed study of the topics

related to the proposed system. This literature survey helped to identify different approaches to implement the related systems, their methodology, pros & cons of each approach etc.

Chapter 3

Methodology

3.1 Introduction

This chapter explains various methodologies that were used in gathering data and analysis of existing systems in the field of PV based boost with bidirectional battery charger, bidirectional converters and H bridge inverter topologies. The methodologies will include areas such as collecting information on existing systems after the idea origin, detailed study on limitations of those, inculcate new ideas to replace the existing ones, and finally the development of new idea to implementation level.

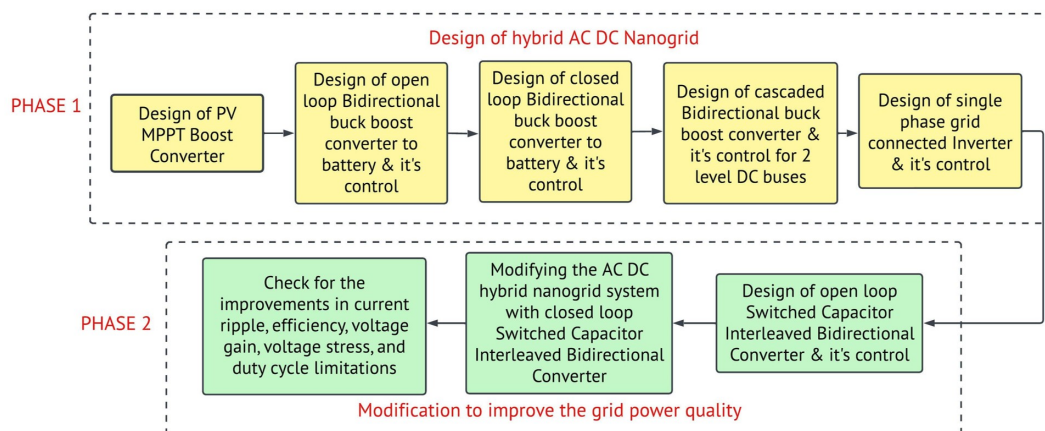


Fig. 3.1: Methodology

3.2 Research on existing systems

Detailed literature survey is done on IEEE journals and conference papers dealing with similar topic. The disadvantages of these systems were identified and is improved in the modified system.

3.3 Proposed system

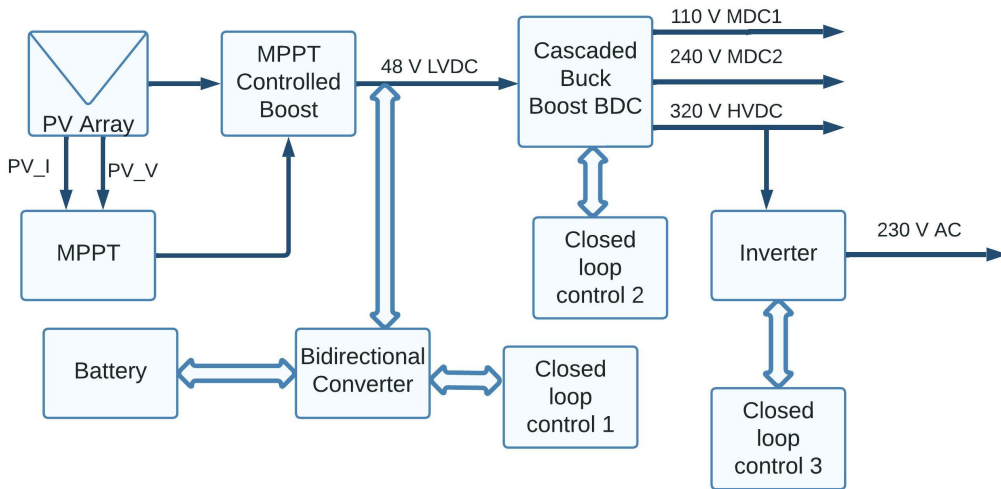


Fig. 3.2: Proposed System

The project is proposing four different level DC buses i.e 48 V (LV), 110 V (MV), 240 V (MV) , 320 V (HV) and an AC bus(230 V, 50 Hz) in the hybrid nanogrid. The four different levels of DC is for different rated DC loads and the AC bus is for powering the conventional AC loads. This can be achieved by using a Boost converter, bidirectional buck boost converter, cascaded buck boost bidirectional converter and a H bridge inverter.

The low voltage DC link and the battery are both charged while the PV's output is increased to 48 V. The cascaded bidirectional buck boost converter utilises this as its input and outputs two levels of DC voltage for MV and HV buses. The single phase H bridge inverter uses the high voltage as input to create 230 V AC to supply the grid.

3.4 Design of PV MPPT Boost Converter

The PV MPPT Boost component parameters are designed and simulated in Matlab. Redesigning of simulation parameters are done to achieve the required output. MPPT algorithm used is Incremental Conductance.

3.4.1 PV Array Sizing

Total load = 15 kW

We multiply the backup hours by the total watts of the load that needs to be turned on to compute the watt hour:

Watt hour = watts \times hrs/day

Total load in Wh = 15 kW \times 10 = 150KWh

Installing a 130 Wh capacity is required to satisfy the appliance's energy requirement of 100 Wh in order to make up for the power lost in the wires, battery, and controller (multiply appliance watt hour demand by 1.3 to install the desired capacity of the PV system panels or modules)

Panel energy = Wh \times 1.3,

Panel energy = 1.3 \times 150 kWh = 195 kWh/day

Calculating the panel generation factor is necessary to make up for environmental impacts,

Table 3.1: Panel generation factor

Desert Area	3.86
Land Area	3.43
Cloudy area (5-7 days/month)	3.00
Cloudy area (<10 days/month)	2.57

Peak panel power = Wh \div PGF,

Peak panel power = 195 kWh \div 3:43 = 56851Wh = 5685.1 watts

For a 250 W panel,

Maximum power PM

$$P_M = V_M \times I_M$$

$$P_M = 30.6 \text{ V} \times 8.17 \text{ A} = 250 \text{ W}$$

Calculate the number of modules to be connected in series and parallel,

$$N_S = V_{MA} / V_M = 150 / 30.6 = 4.9 \text{ (Higher integer value 5)}$$

$$V_{MA} = V_M \times N_S = 30.6 \times 5 = 153 \text{ V}$$

$$N_P = I_{MA} / I_M = 38 / 8.17 = 4.65 \text{ (Higher integer value 5)}$$

$$I_{MA} = I_M \times N_P = 8.17 \times 5 = 40.85 \text{ A}$$

Calculating the total power of the PV array

$$P_{MA} = N_S \times N_P \times P_M = 5 \times 5 \times 250 = 6250 \text{ W}$$

Thus, we need 25 PV modules.

A string of 5 modules connected in series and 5 such strings connected in parallel, having a total power of 6250 W at maximum PV array current and voltages of 40.85 A and 153 V respectively.

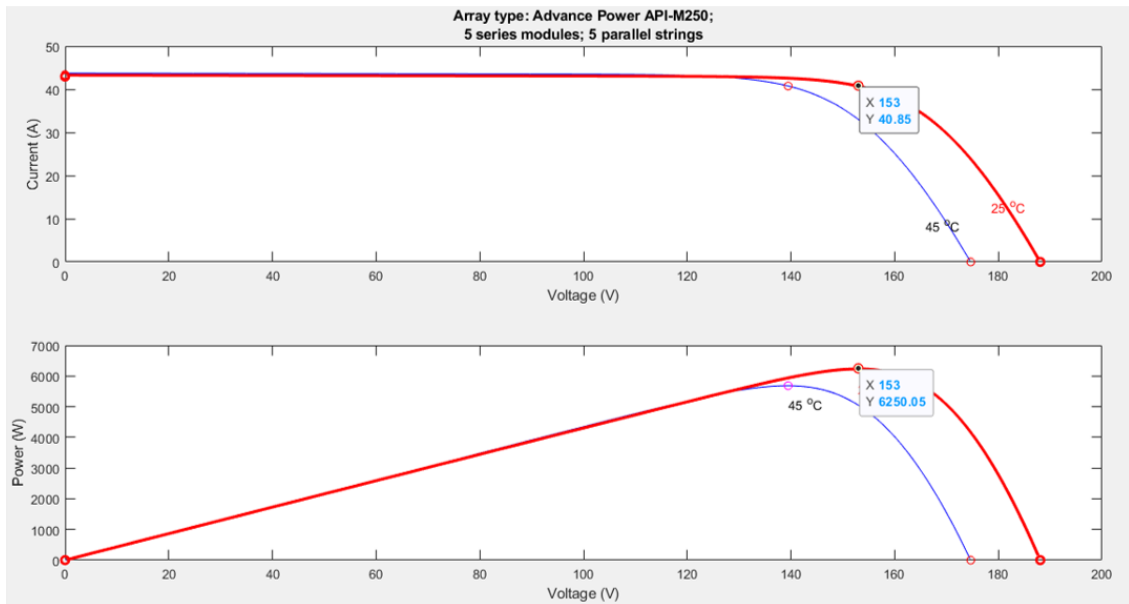


Fig. 3.3: PV Characteristics

3.4.2 MPPT Control design

Grid-tie inverters, solar battery chargers, and other similar devices use the maximum power point tracking (MPPT) method to extract as much electricity

as they can from one or more solar panels. The complicated connection between solar radiation, temperature, and total resistance in solar cells results in the I-V curve, a nonlinear output efficiency. The MPPT system's goal is to sample the cell output and apply the appropriate load (resistance) to get the most power possible under any given climatic circumstances. In incremental Conductance, in order to determine the direction of the change in the power with respect to the voltage (dP/dV), the controller monitors incremental changes in the array current and voltage (dI/dV). Compared to P & O, this technique requires the controller to perform more computation, but it can monitor changing conditions more quickly. The power output may also fluctuate as a result. The MPP voltage is the output voltage when the incremental conductance is zero. Until the irradiation changes and the process is repeated, the controller retains this voltage.

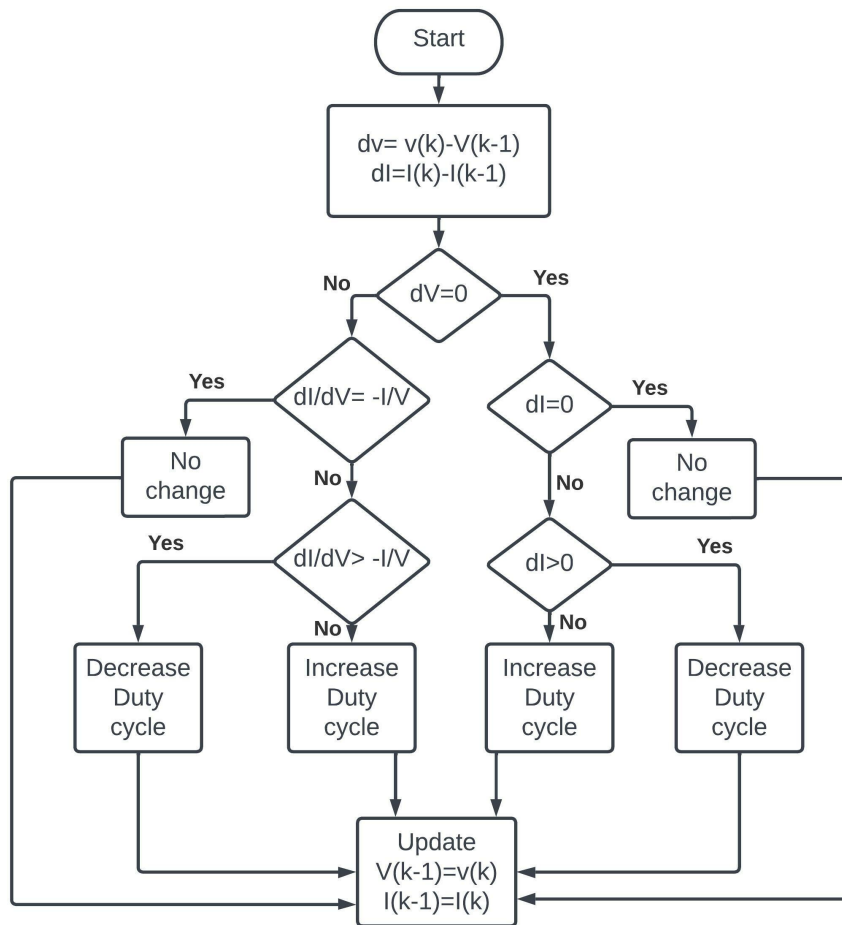


Fig. 3.4: Flowchart of Incremental Conductance

3.4.3 Design of Boost Converter

Desired output, $V_o=48$ V

1. Selection of d

$$d_{min} = 1 - \frac{V_{in_min}}{V_o} = 0.625 \quad (3.1)$$

$$d_{max} = 1 - \frac{V_{in_max}}{V_o} = 0.5625 \quad (3.2)$$

Nominal d=0.6

2. Inductor Ripple Current, ΔI_L

$$\Delta I_L = (0.2 - 0.4) \times I_{out_max} \times \frac{V_o}{V_{in}} = 0.8 \quad (3.3)$$

3. Selection of L_{min}

$$\Delta I_L \geq \frac{d(1-d) \times V_o}{f_s \times L} \quad (3.4)$$

$$L_{min} = 1.8mH$$

4. Selection of Output capacitance

$$C_{out} = \frac{I_{out_max} \times d}{f_s \times \Delta V_o} = 2200\mu F \quad (3.5)$$

3.5 Design of Bidirectional Buck boost converter to battery & Cascaded bidirectional converter

The component parameters are designed and simulated in Matlab and are redesigned to achieve the desired output. The control system for both the converters are designed and simulated for the closed loop operation using PI controller.

3.5.1 Design of Bidirectional Buck boost Converter

Desired output , $V_o=24$ V Nominal input , $V_{in}= 48$ V

Forward operation (Buck mode)

Desired output , $V_o=24$ V Nominal input , $V_{in}= 48$ V

1. Duty Cycle (d)

$$d = \frac{V_o}{V_{in} \times \eta} = 0.6 \quad (3.6)$$

2. Selection of inductor

$$\Delta I_L = (0.1 - 0.2) \times I_{out} = 2.5A \quad (3.7)$$

$$L = \frac{d \times (V_{in} - V_o)}{f_s \times \Delta I_L} = 0.5mH \quad (3.8)$$

Backward operation (Boost mode)

Desired output , $V_o= 48$ V Nominal input , $V_{in}= 24$ V

1. Duty Cycle (d)

$$d = 1 - \frac{V_{in} \times \eta}{V_o} = 0.6 \quad (3.9)$$

2. Selection of inductor

$$\Delta I_L = (0.1 - 0.2) \times I_{in} = 2.5A \quad (3.10)$$

$$L = \frac{d \times V_{in}}{f_s \times \Delta I_L} = 0.5mH \quad (3.11)$$

3. Selection of Output capacitance

$$\Delta I_L = \frac{I_o}{1 - d} = 2.5A \quad (3.12)$$

$$C_{out} = \frac{I_o \times d}{f_s \times \Delta V_o} = 2200\mu F \quad (3.13)$$

3.6 Design of Grid connected H bridge inverter

The H bridge inverter with its controller is designed and simulated to get a synchronized output ready to be fed back to the utility.

3.7 Switched Capacitor Interleaved Bidirectional Converter

The Switched Capacitor Interleaved Bidirectional Converter can supply the constant dc bus voltage due to its broad voltage-gain range. Additionally, a three-phase interleaved structure built on switched-capacitor cells significantly lowers the voltage stresses across the power switches and the current ripple on the LVS. The input and output of the switched-capacitor interleaved bidirectional (SCIB) converter have an absolute common ground. Therefore, a wide range of voltage gain, decreased current ripple and voltage stress on the power switches, and good topology scalability are the primary benefits of the SCIB converter.

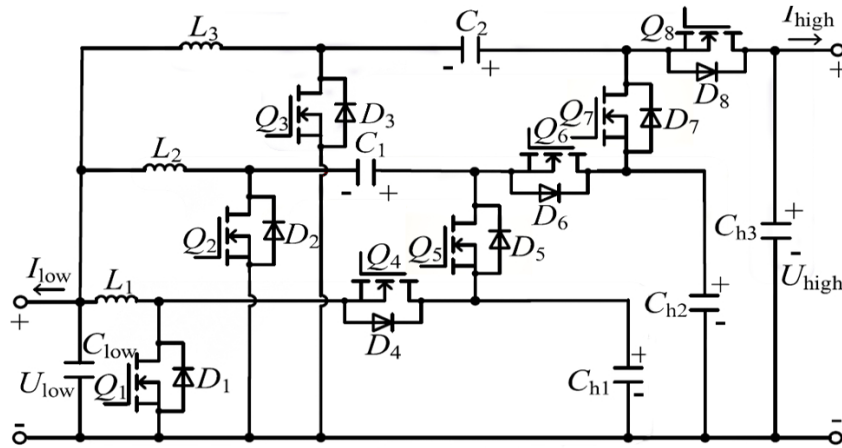


Fig. 3.5: SCIB Converter configuration

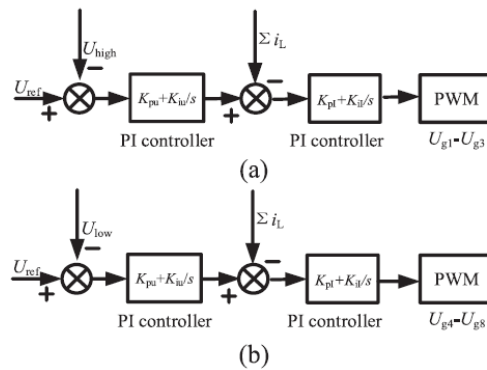


Fig. 3.6: Double loop control diagram. (a) Step-up mode (b) Step-down mode

A basic buck/boost network (L_1, Q_1, Q_4 & C_{h1}) and two extended buck/boost networks (L_2, Q_2, C_1 and Q_6) make up the SCIB converter's configuration. Power switches Q_5, Q_7, C_{h2} and $L_3, Q_3, C_2, Q_8, C_{h3}$, energy storage/filter capacitance C_{low} on the LVS. The SCIB converter allows for bidirectional power transfer between the HVS and LVS by operating in either the step-up or step-down mode.

3.7.1 Modes of operation

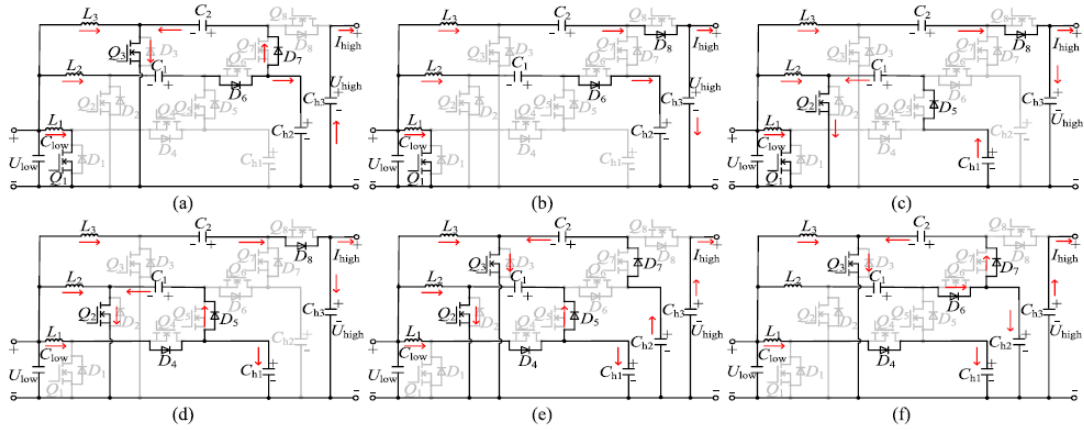


Fig. 3.7: Current-flow paths in the step-up mode

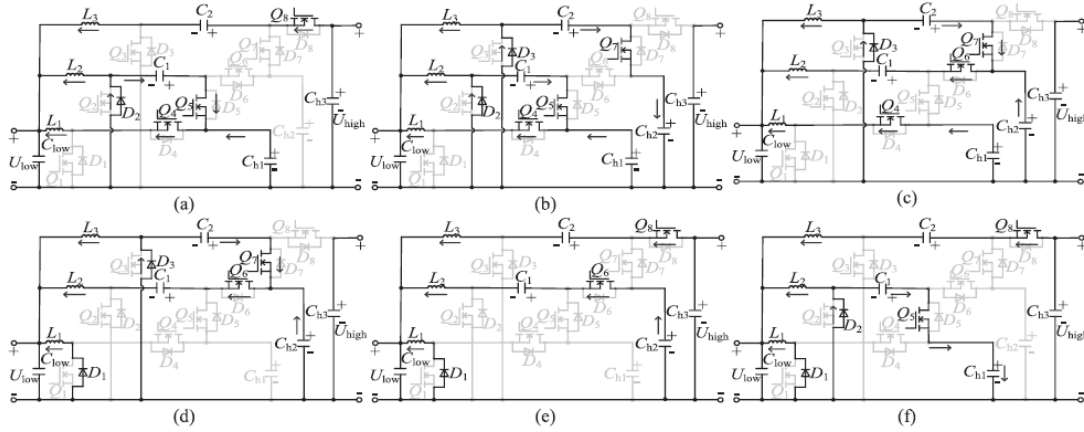


Fig. 3.8: Current-flow paths in the step-down mode

3.7.2 Design

1. Selection of inductance of the inductors L1–L3

$$L_1 = L_2 = L_3 = \frac{U_{low}d_{boost}}{f_s\Delta I_L} \quad (3.14)$$

2. Selection of capacitance of the capacitors C_1 and C_2

$$C_1 \geq \frac{(1 - d_{boost})I_{L2}}{f_s \Delta U_{C1}} = 246 \mu H \quad (3.15)$$

$$C_2 \geq \frac{(1 - d_{boost})I_{L3}}{f_s \Delta U_{C2}} = 238 \mu H \quad (3.16)$$

3. Selection of capacitance of the capacitors C_{h1} and C_{h2}

C_{h1} and C_{h2} are identical to C_1 and C_2 , respectively, to take the effect of asymmetry out of the equation. Therefore,

$$C_1 = C_2 = C_{h1} = C_{h2} = 270 \mu F \quad (3.17)$$

4. Selection of capacitance of the capacitors C_{h3}

Similar calculations can be used to determine the capacitance of capacitor C_{h3}

$$C_{h3} \geq \frac{(1 - d_{boost})I_{high}}{f_s \Delta U_{high}} = 238 \mu H \quad (3.18)$$

3.8 Proposed system modification

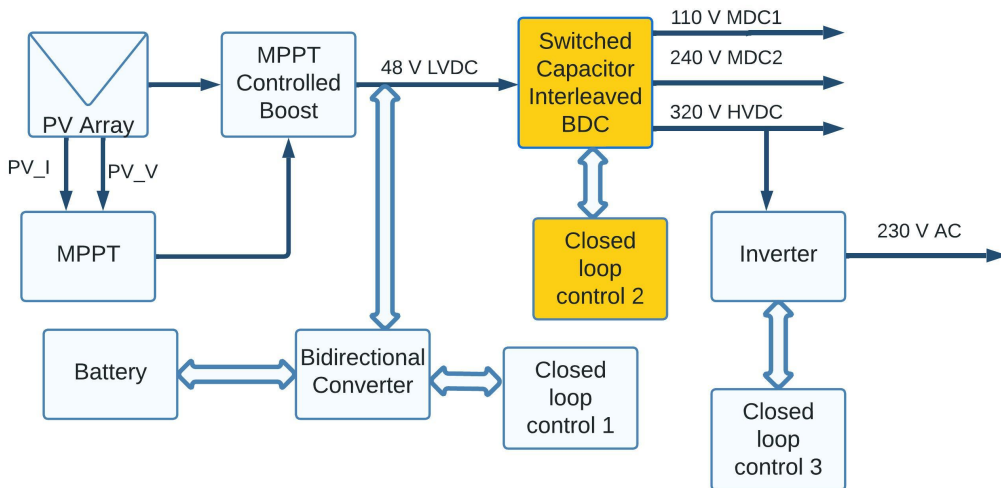


Fig. 3.9: Proposed System modification

The modified system is proposing four different level DC buses i.e 48 V (LV), 110 V (MV) , 240V(MV), 320 V (HV) and an AC bus (230 V, 50 Hz)

in the hybrid nanogrid. The modified system replaces the cascaded buck boost bidirectional converter with Switched capacitor interleaved bidirectional converter in order to reduce ripples & voltage stress and to improve the efficiency & voltage gain.

The output of the PV is boosted to 48 V, the low voltage DC bus and also charge the battery. This is fed as the input to the switched capacitor interleaved bidirectional converter which gives out three levels of DC voltages for two MV and one HV buses. The high voltage act as input to the single phase H bridge inverter that produces 230 V AC and will feed the grid.

3.9 Conclusion

The complete proposed system is initially individually developed and simulated and then incorporated together to achieve the different DC Voltage buses and the AC bus in phase I. Then, the proposed system is modified with new converter and is checked for improvements in phase II.

Chapter 4

Simulation

4.1 Introduction

Matlab Simulink is used for simulation. The math computing environment and proprietary multi-paradigm computer language MATLAB were created by MathWorks. MATLAB is an acronym for "MATrix LABoratory." Matrix manipulation, function and data plotting, algorithm implementation, user interface creation, and interfacing with other programming languages are all possible with MATLAB.

Although MATLAB is mainly designed for numeric computation, symbolic computation capabilities are accessible through an optional toolbox that uses the MuPAD symbolic engine. Graphical multi-domain modelling and model-based design for embedded and dynamic systems are added by an additional package called Simulink.

4.2 PV MPPT Boost Converter

The output of the PV is fed as the input to the boost converter which boosts the input voltage to required LVDC bus voltage i.e 48 V. The gate pulse from the Incremental conductance algorithm control the PWM generator of the Boost converter switch.

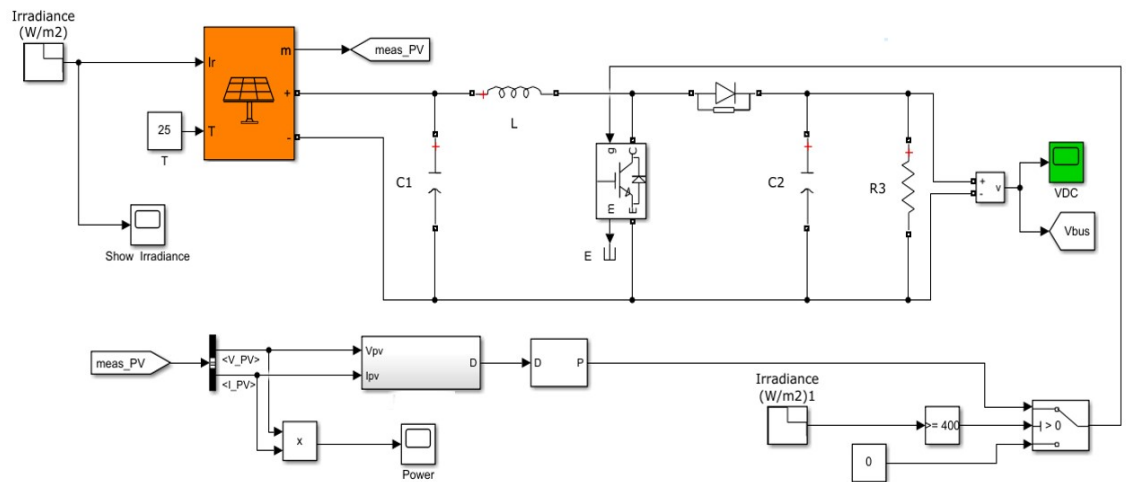


Fig. 4.1: PV MPPT Boost Converter

4.2.1 MPPT Control

```

1 function y = MYMPP(u,i,uo,io,D)
2 m=0.4;
3 du=u-uo;
4 di=i-io;
5 d=0.00005;
6 if du==0
7     if di==0
8         m=D;
9     else
10        if di>0
11            m=D-d;
12        else
13            m=D+d;
14        end
15    end
16 else
17     if di/du== -(i/u)
18         m=D;
19     else
20         if di/du> -(i/u)
21             m=D-d;
22         else
23             m=D+d;
24         end
25     end
26 end
27 y = m;
28 end
    
```

Fig. 4.2: Incremental Conductance algorithm

The PV module's output is always fluctuating. An MPPT is used with the DC-DC converter to get the maximum power out of the panel. The Matlab embedded block is then modified by adding the MPPT algorithm to create the MPPT block. The output of the MPPT, i.e the duty cycle is fed to the mosfet of the DC-DC boost converter, while the output of the PV module's current and

voltage are passed into the Matlab embedded block.

The P-V curve’s slope is picked up by the incremental conductance algorithm, and the P-V curve’s extreme is utilized to find the MPP. For MPPT, this algorithm employs the incremental conductance dI/dV and the instantaneous conductance I/V . The MPPT function block’s output, a duty cycle, is passed to the PWM generator to produce the gate pulse for the boost converter’s mosfet.

4.3 Bidirectional buck boost converter

If irradiance in the PV is greater than 400 W/m^2 , then simultaneously the DC bus is powered with 48 V boost output and at the same time the battery is charged. The 48 V is bucked to charge the battery. If irradiance in the PV is less than 400 W/m^2 , then the boosting operation stops and the 48 V LVDC bus is fed from the battery after boosting the battery output to 48 V by the bidirectional converter. So the forward mode of the bidirectional buck boost converter is buck mode and the backward mode is boost mode. Thus the BDC act as buck when irradiance in the PV is greater than 400 W/m^2 and as boost when it is less than 400 W/m^2 .

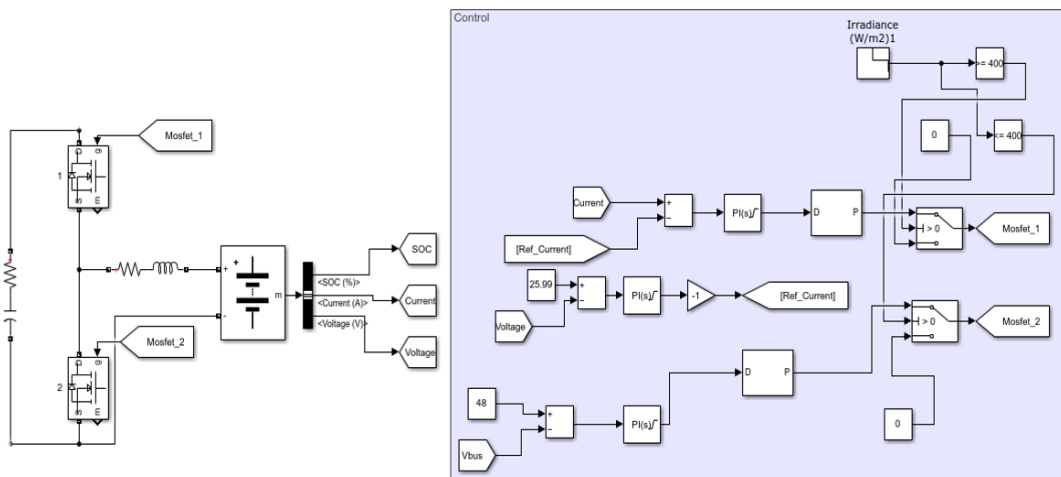


Fig. 4.3: Battery bus with bidirectional buck boost converter and its control

Battery voltage and the required cut off voltage is given to a PI controller to produce the reference current. This reference current is compared with the

battery current and duty cycle is generated. From this duty cycle, PWM pulses are generated, which is given to the upper MOSFET switch during buck operation. During boost mode, 48 V reference is compared against the LVDC bus volatge with a PI controller which generates the required duty cycle.

4.4 Cascaded Bidirectional buck boost converter

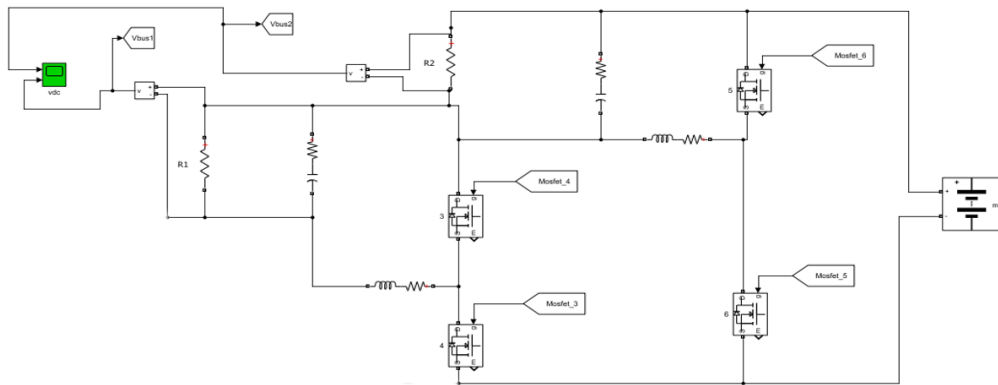


Fig. 4.4: Battery bus with cascaded bidirectional buck boost converter

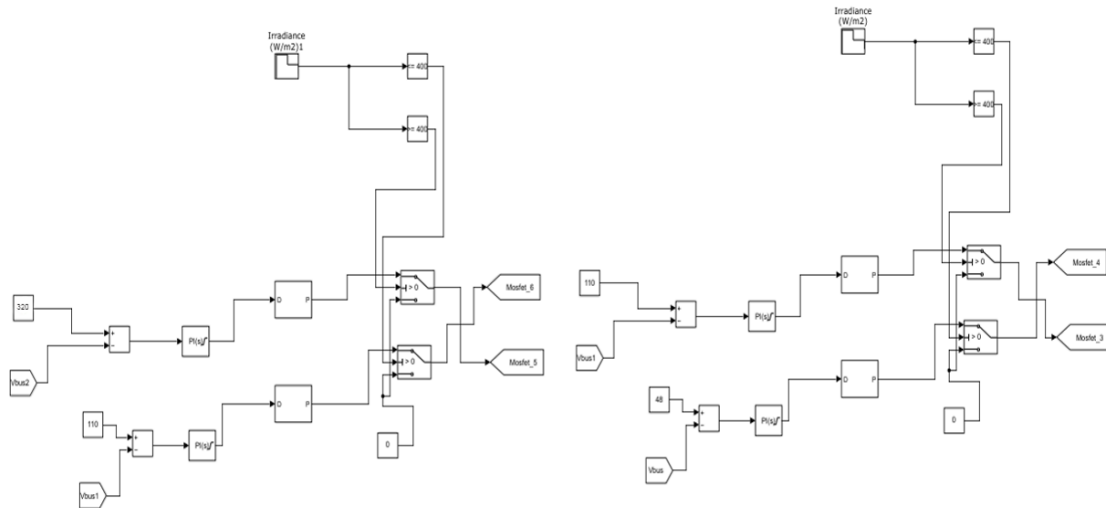


Fig. 4.5: Cascaded bidirectional buck boost converter control

The Cascaded Bidirectional buck boost converter act as boost in forward operation with the lower mosfets acting as switch while it act as buck converter in backward operation mode with the upper mosfets as switch. The forward and backward mode is controlled by the irradiance value. It requires two PI controllers

for this operation. The output of this converter is two DC buses 110 V (MV) and 320 V (HV).

4.5 Grid connected single phase H bridge Square wave Inverter

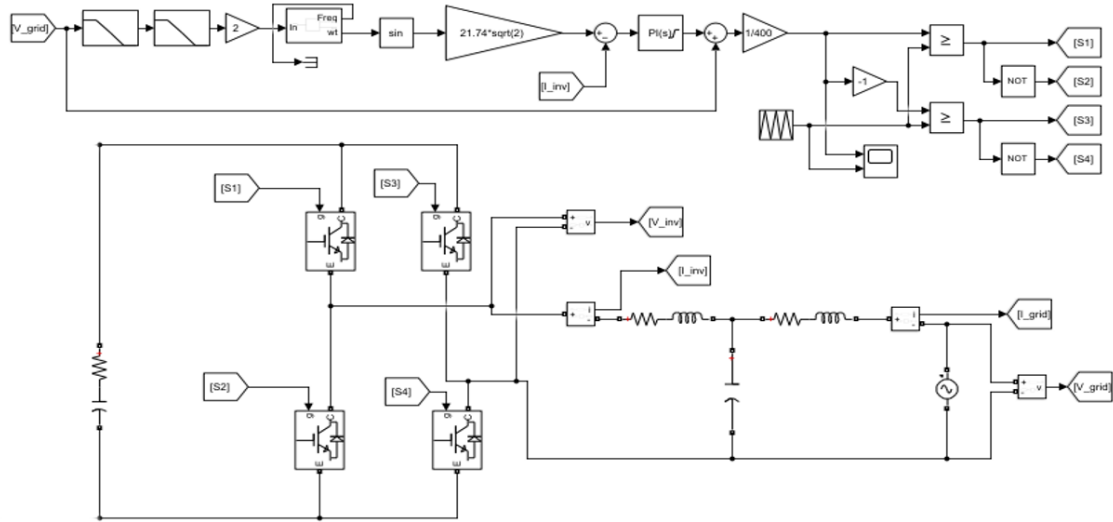


Fig. 4.6: Grid connected single phase H bridge square wave Inverter with its control

This Voltage source inverter is fed with a 320V DC and is converted to 230 V AC. This generates a square AC wave of 230 V RMS value which is synchronised with the grid voltage and current using the control circuit. The grid voltage i.e 230 V, 50 Hz AC is given as input to the control circuit. It passes through the low pass filters to filter out the higher order harmonics, which is then fed to the Phase locked loop(PLL). A control system that produces an output signal whose phase is correlated to the phase of an input signal is known as a phase-locked loop (PLL). A phase detector and a variable frequency oscillator operate in a feedback cycle to form the PLL. Voltage-controlled oscillators (VCO) are so named because the frequency and phase of the oscillator are proportionally regulated by the applied voltage. In order to maintain the phases matched, the oscillator generates a periodic signal with a specific frequency, and the phase detector compares the phase of that signal with the phase of the periodic signal input. Maintaining the same input and

output frequencies also entails maintaining the input and output period in lockstep. Consequently, a phase-locked loop can monitor an input frequency in addition to synchronising signals. Using a PI controller, the sine of the phase angle output is multiplied by the peak value of the grid current before being compared with the inverter current and fed back into the low pass filter. The H bridge inverter's switching pulses are produced in the subsequent part of the control circuit. For this, sinusoidal PWM is employed. To create the switching pulses, the output from the PI controller is compared with the triangular wave. This causes S1 and S4 to be turned ON simultaneously for the positive half of the cycle, while S2 and S3 are used for the negative half. As a result, the grid output and square AC output will be synchronised.

4.6 Grid connected single phase H bridge sine wave Inverter

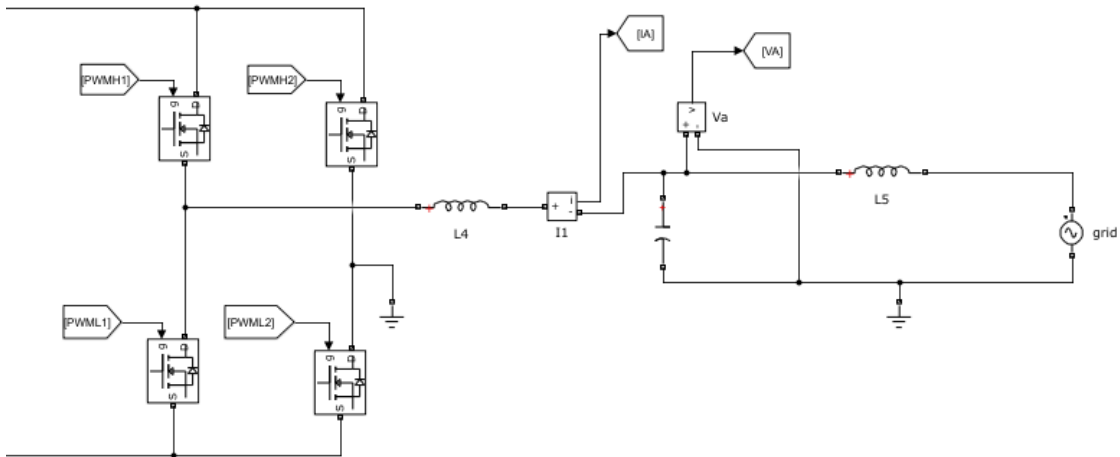


Fig. 4.7: Grid connected single phase H bridge sine wave Inverter

A 320V DC is fed into this voltage source inverter, which produces 230 V AC. By employing the control circuit, this generates a square AC wave with a 230 V RMS value that is synchronised with the grid voltage and current. The input to PLL is the inverter voltage. A phase-locked loop is a type of control system that

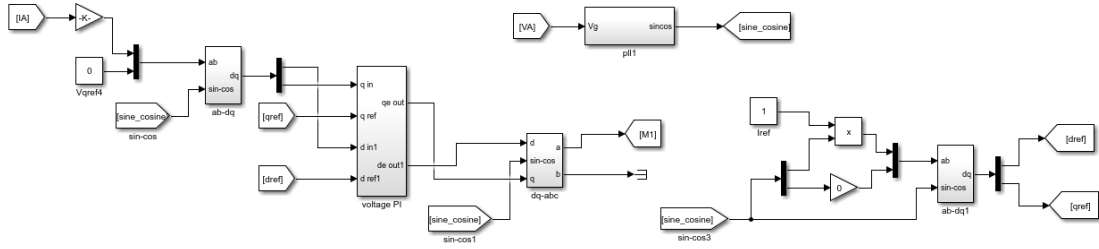


Fig. 4.8: H bridge sine wave Inverter control

generates an output signal whose phase is associated to the phase of an input signal. (PLL). The PLL is composed of a phase detector and a variable frequency oscillator that work in a feedback loop. The word "voltage-controlled oscillator" (VCO) refers to an oscillator whose frequency and phase are proportionally controlled by the applied voltage. The oscillator produces a periodic signal at a certain frequency, and the phase detector checks the phase of that signal with the phase of the periodic signal input in order to keep the phases aligned. The input and output period must be kept in lockstep in order to retain the identical input and output frequencies. Inverter current and PLL output is used for the transformation of inverter current in the abc frame to the dq frame using the park transformation. As the dq-frame only needs two compensators, this conversion decreases the number of compensators needed. Additionally, because the reference signal in an abc-frame is sinusoidal, you cannot utilise PI controllers as your compensator and must instead develop compensators that accurately follow your reference signal, which can be challenging as system complexity rises. A PI controller can be utilised as a compensator because controlling in a dq-frame is the same as managing DC quantities. Two PI controllers receive the converted dq frame values and compare them to the reference dq values. After that, the PI's regulated output is once more transformed to the abc frame, which creates the pulses needed to turn the inverter. For the positive half of the cycle, S1 and S4 are simultaneously switched ON, whilst S2 and S3 are employed for the negative half. The output of the grid and the output of the sinusoidal AC inverter will thus be synced.

4.7 Switched capacitor interleaved bidirectional converter

The SCIB converter simulation is shown below. The study is made easier by presuming that each component is ideal. Voltages across capacitors are constant, and the on-state resistance R_{DS} of the power switches as well as the corresponding series resistance of the inductors and capacitors are disregarded. The primary power switches $Q_1 - Q_3$ and the freewheeling diodes $D_4 - D_8$ of $Q_4 - Q_8$ are used when the SCIB converter is operating in step-up mode. The duty cycles of the gate signals $S_1 - S_3$ are assumed to be $D_1 = D_2 = D_3 = d_{Boost}$, phase-shifted by 120° in turn. The primary power switches $Q_4 - Q_8$ and the freewheeling diodes $D_1 - D_3$ of $Q_1 - Q_3$ are used when the SCIB converter is in the step-down mode. The duty cycles for the gate signals $S_4 - S_8$ are $d_4 = d_6 = d_8 = d_{Buck}$ and $d_5 = d_7 = 1 - d_{Buck}$, respectively. $S_4, S_6,$ and S_8 are also phase-shifted by 120° in turn. S_5, S_7 are complementary to S_6, S_8 .

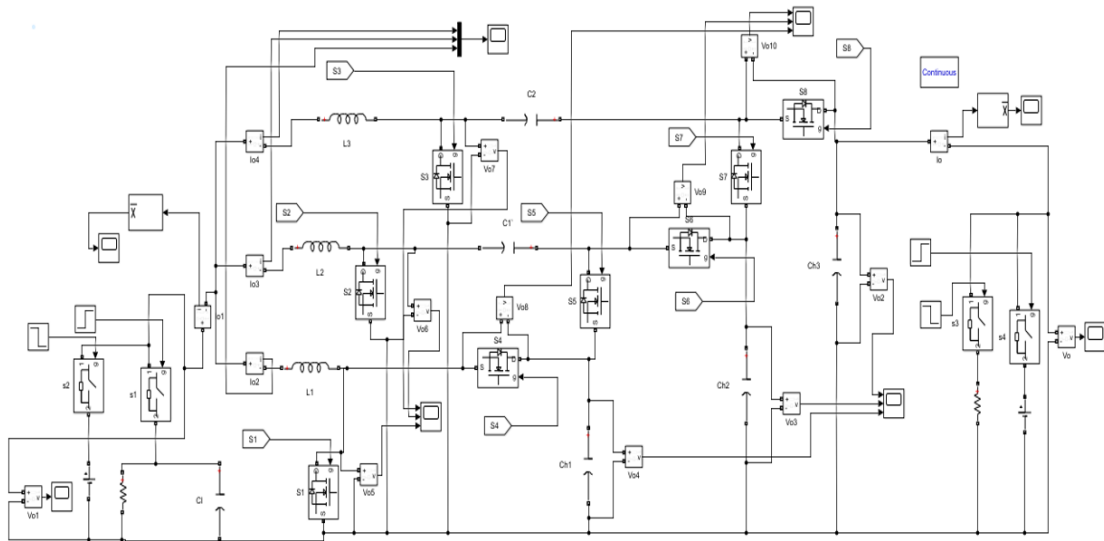


Fig. 4.9: Switched capacitor interleaved bidirectional converter

In open loop system, in order to produce the gate signals for the power switches in both bucking and boosting modes of operation, the absolute value of the triangular pulse is compared to the fixed duty cycle. Additionally, a 120° phase change

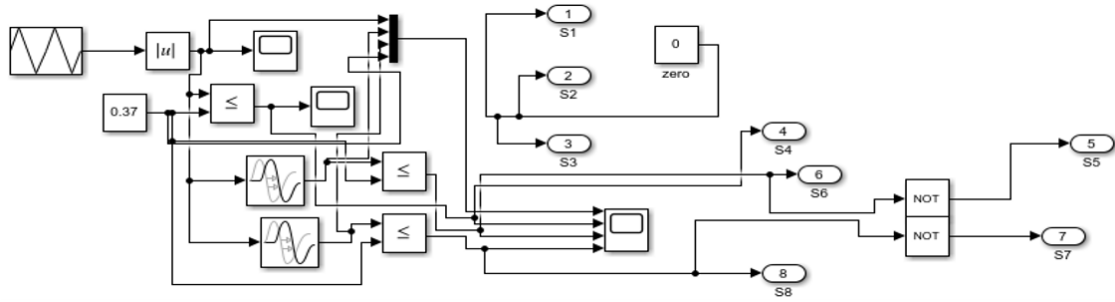


Fig. 4.10: Open loop control of SCIB converter in buck mode

is applied in turn to the necessary switches using a transportation delay block. The phase delay is used to determine the time delay for the pulses to be used in the transportation delay block in Simulink.

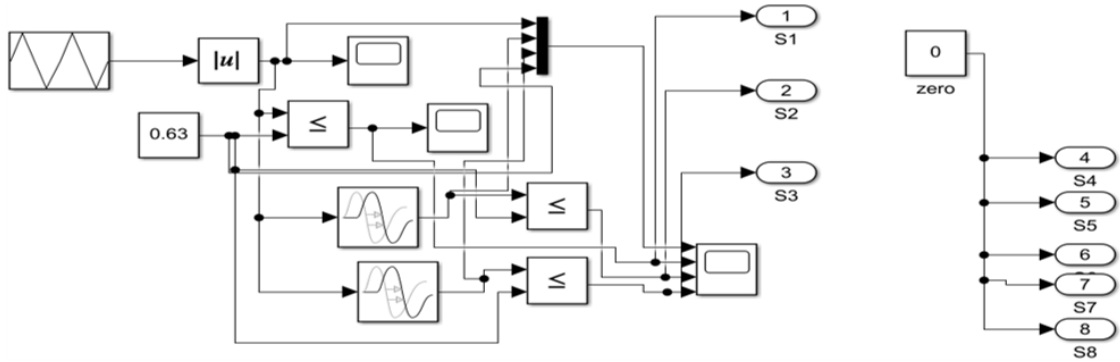


Fig. 4.11: Open loop control of SCIB converter in boost mode

In contrast to an open loop control system, where the duty cycle was fixed, a closed loop control system compares the absolute value of the triangular pulse to the duty cycle generated by the PI controller to produce the gate signals for the power switches in both step up and step down modes of operation. The double loop control system is used to produce the duty cycle from the PI controller. For step-up mode, the PI controller compares the HV bus voltage to the required HV voltage, and then uses an additional PI controller to compare the output of the former PI to the current from the HV bus. To maintain the bus voltage constant, the PI controller will produce the duty cycle.

In the step-down mode, the same procedure is followed, but in this instance, the reference value and comparing values will be of the LV bus.

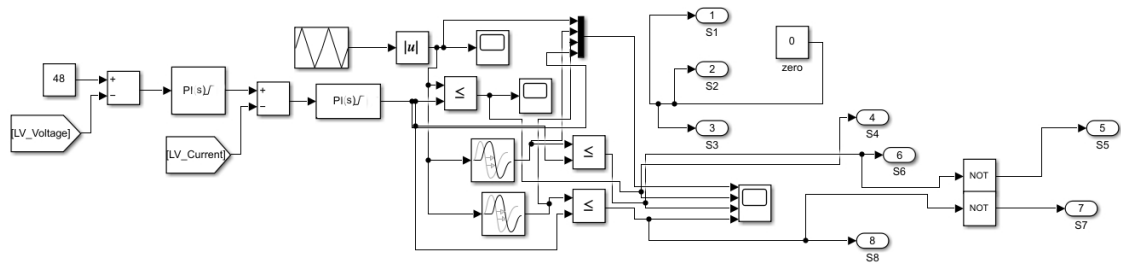


Fig. 4.12: Closed loop control of SCIB converter in buck mode

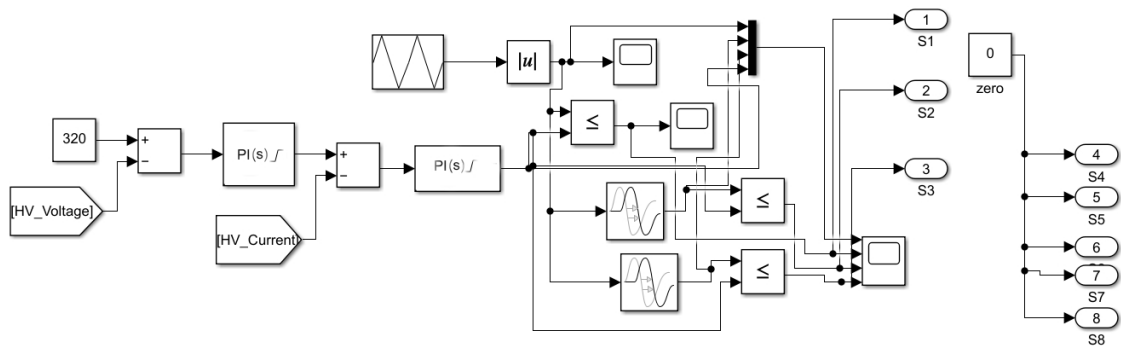


Fig. 4.13: Closed loop control of SCIB converter in boost mode

4.8 Conclusion

The simulation of the proposed system and modified system are carried out in Matlab and the results are analysed to find the ripple, voltage stress, THD etc. The two results are compared.

Chapter 5

Results and Discussions

5.1 Introduction

This section incorporates the results of the proposed system and modified system simulation with different levels of irradiation to the PV.

5.2 Results with Cascaded buck boost bidirectional converter

The conventional cascaded buck boost converter is designed to get the 3 different levels of DC voltages. The bus currents are also analysed. When the irradiation is changed every one minute in the simulation there is disturbance and it takes around 3 ms to get back to stable condition. The AC generated from the HVDC of the converter is analysed for THD and found to be around 5.77% as shown in fig. 5.9. The voltage stress across the switches are also found to be high. The AC inverter output is found to be synchronized with the grid output, in case of both H Bridge square wave and sine wave inverters.

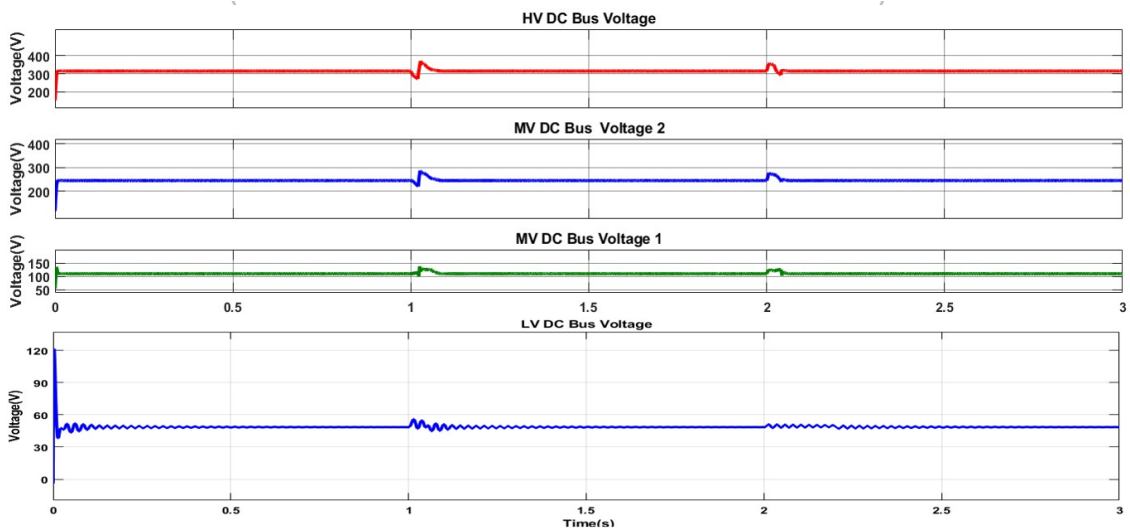


Fig. 5.1: DC Bus Voltages

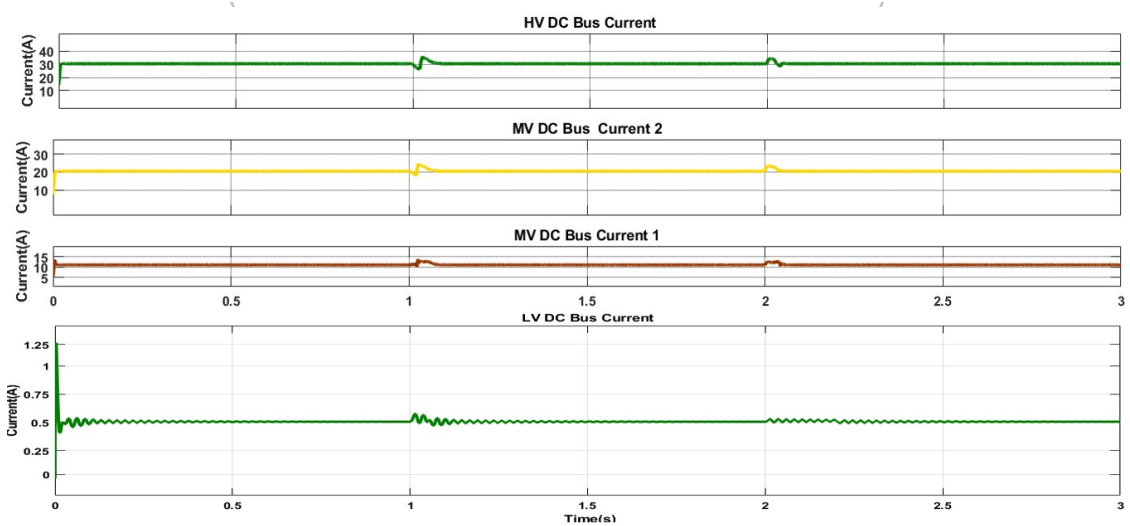


Fig. 5.2: DC Bus Currents

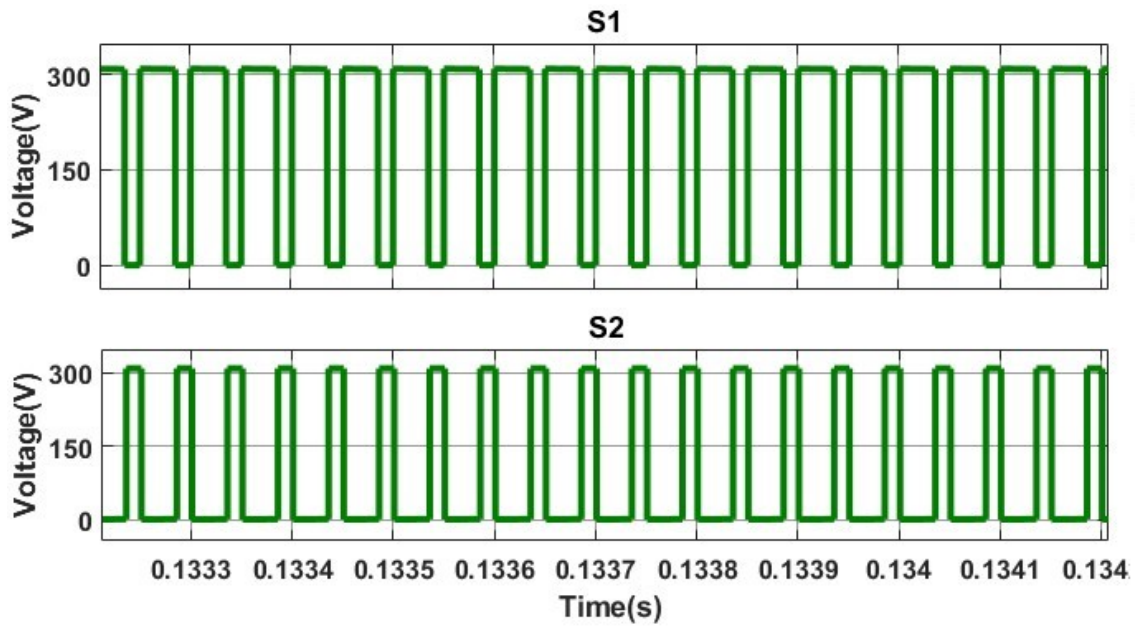


Fig. 5.3: Voltage across switches S1,S2

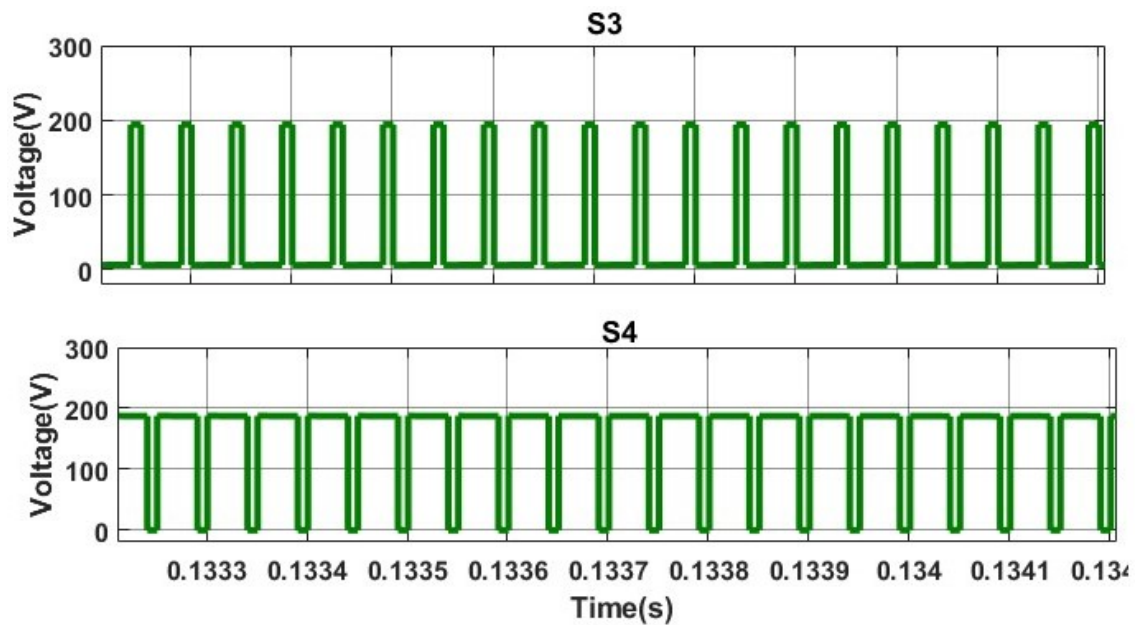


Fig. 5.4: Voltage across switches S3,S4

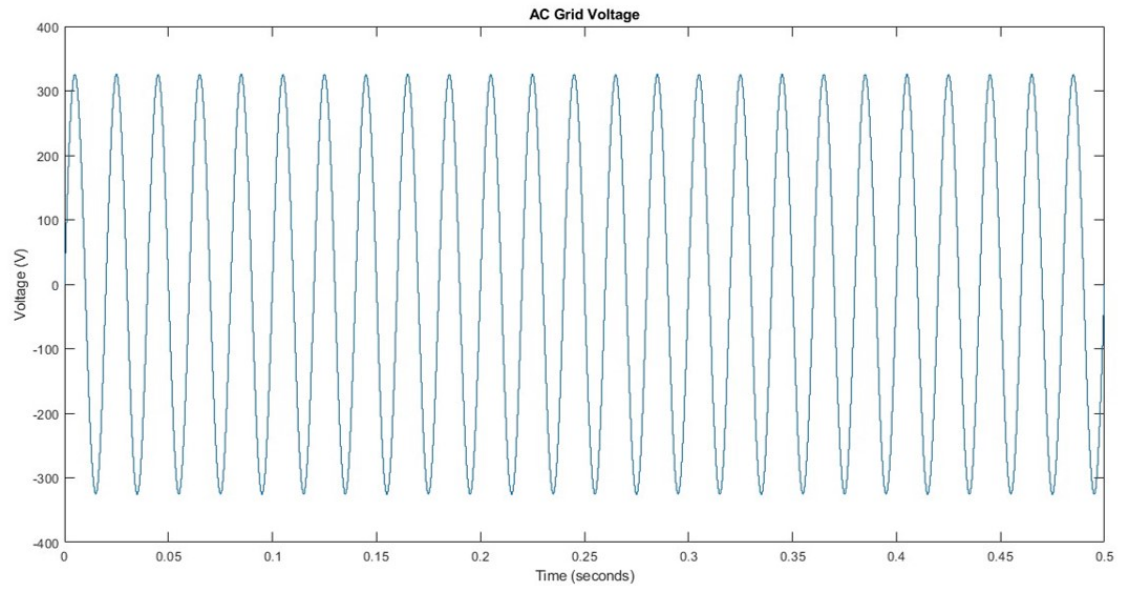


Fig. 5.5: AC grid Voltage

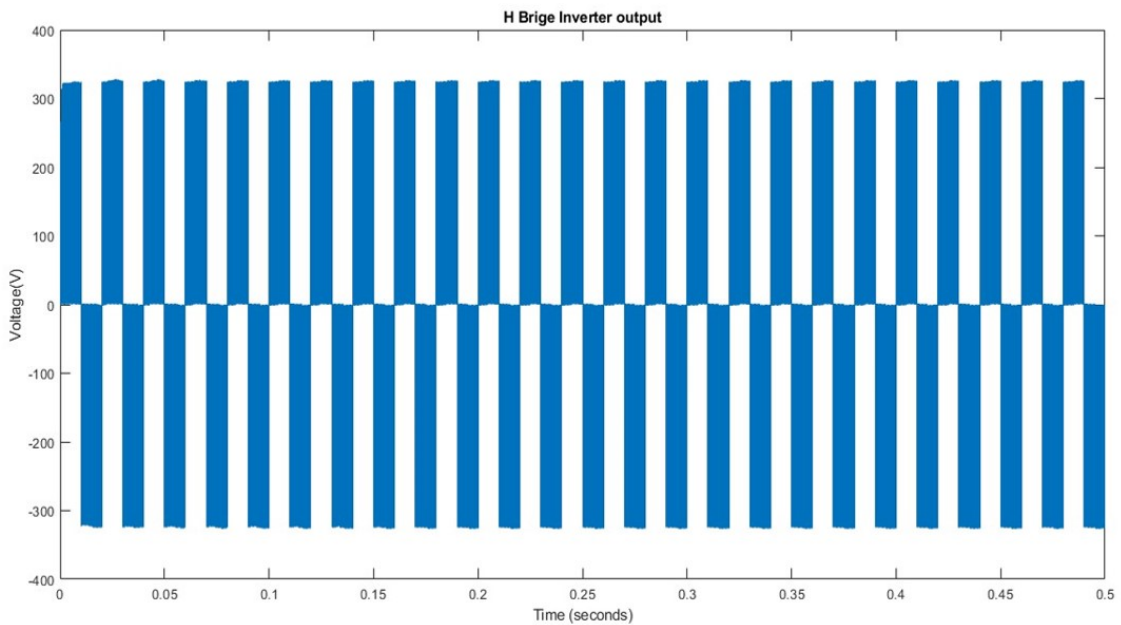


Fig. 5.6: H bridge Square wave Inverter output Voltage

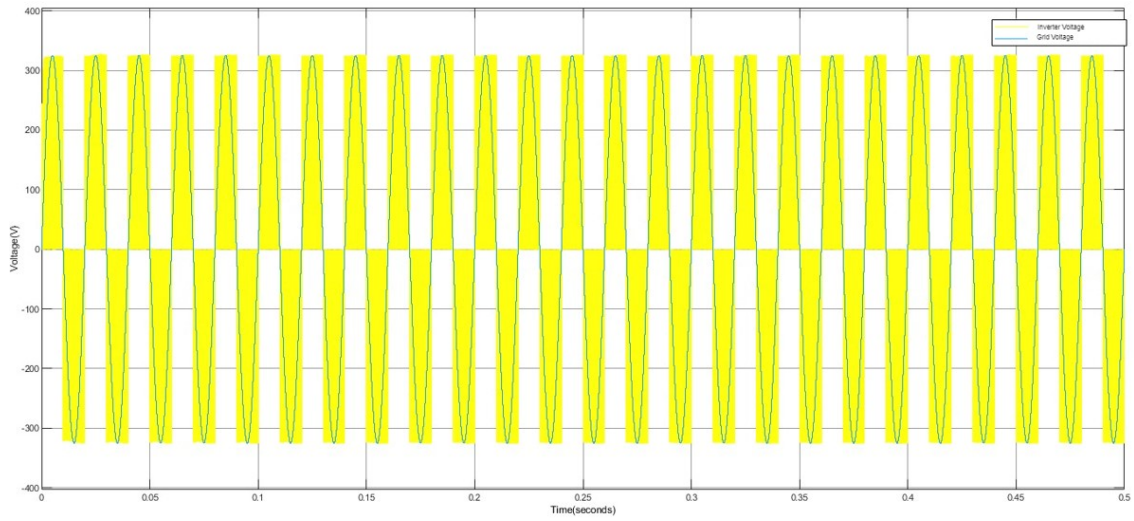


Fig. 5.7: Synchronised AC grid voltage and inverter voltage with square wave inverter

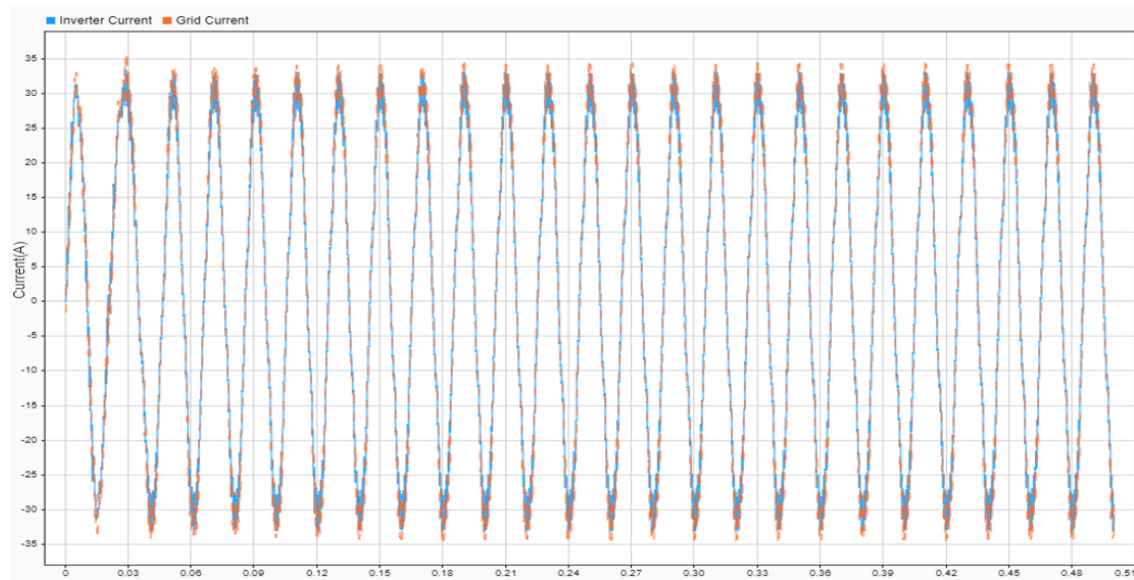


Fig. 5.8: Synchronised AC grid current and inverter current with square wave inverter

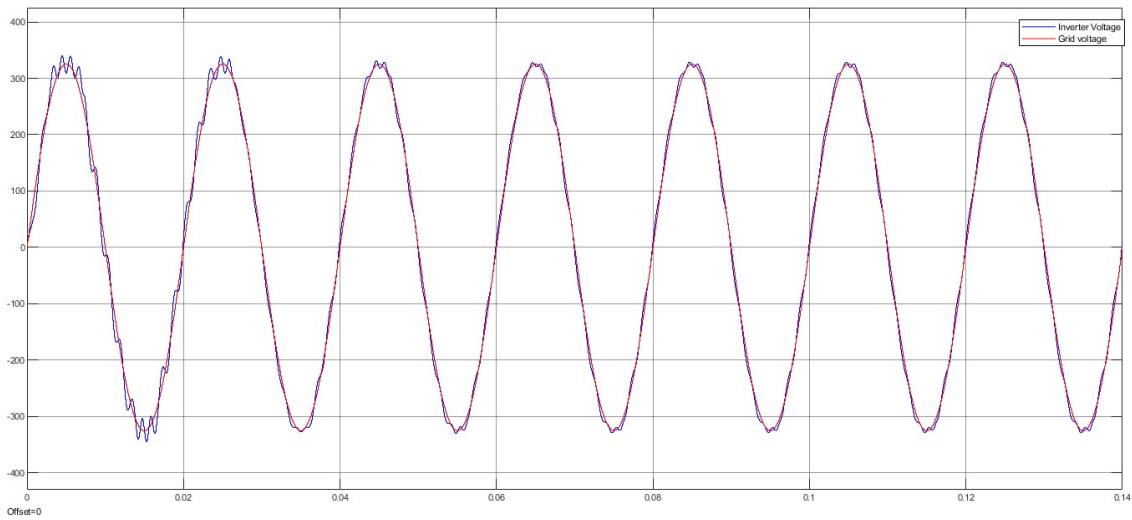


Fig. 5.9: Synchronised AC grid voltage and inverter voltage with sine wave inverter

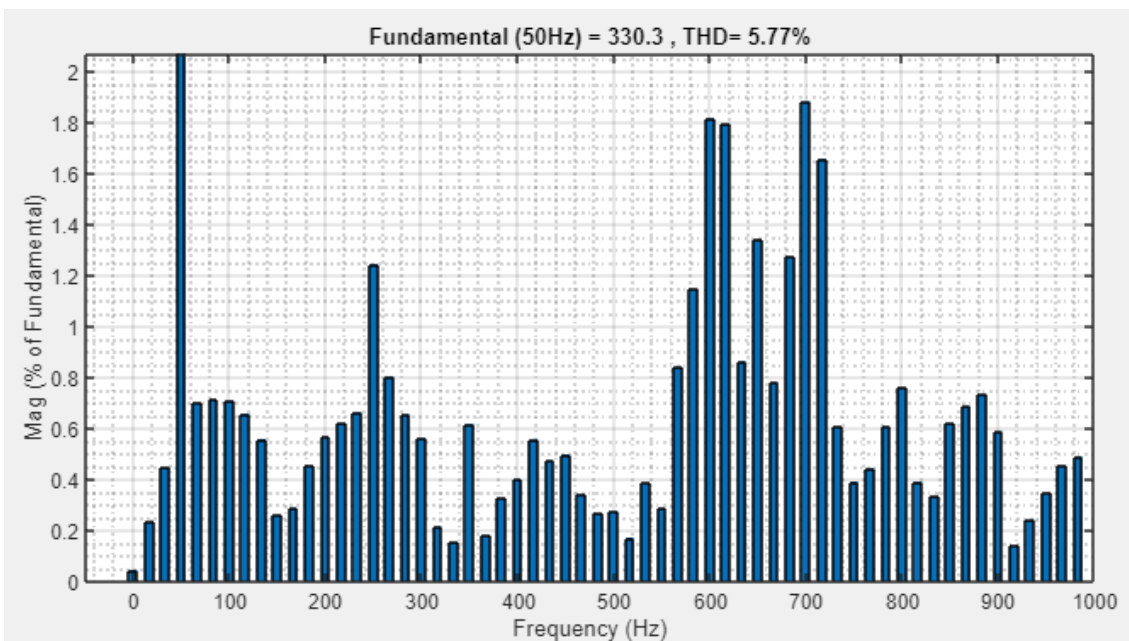


Fig. 5.10: THD Analysis of AC sine wave inverter output

5.3 Results with Switched capacitor interleaved bidirectional converter

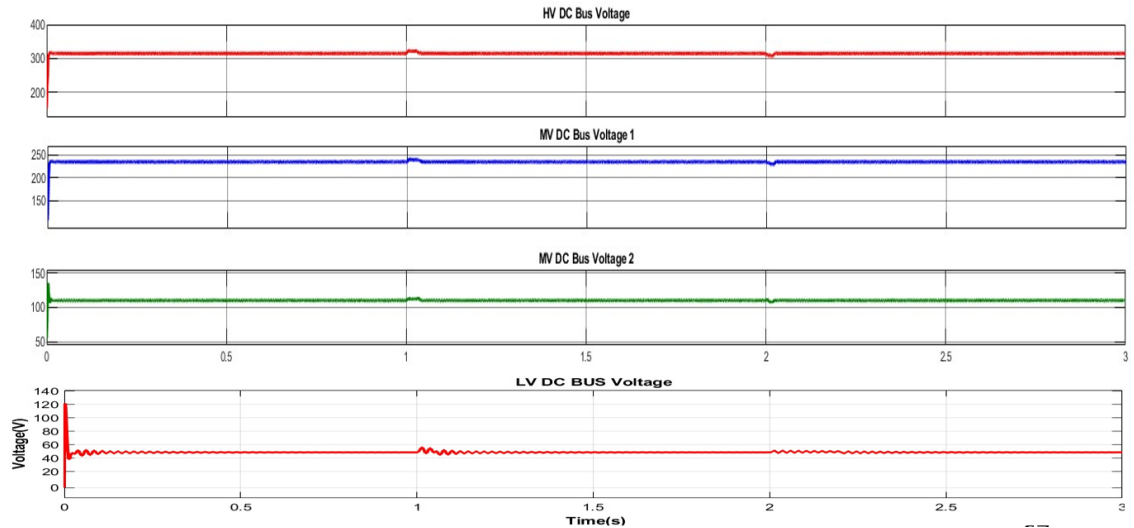


Fig. 5.11: DC Bus voltages

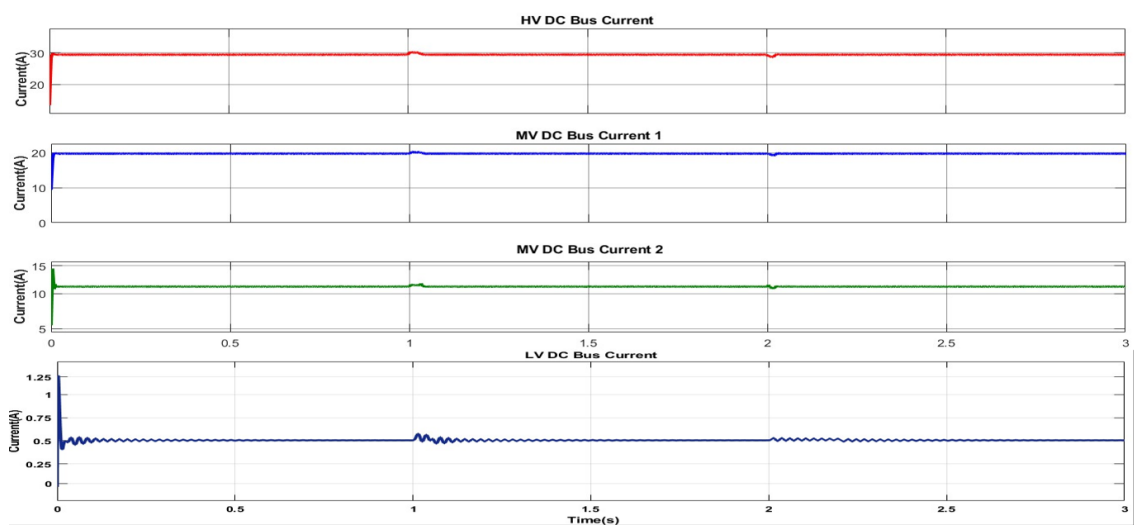


Fig. 5.12: DC Bus Currents

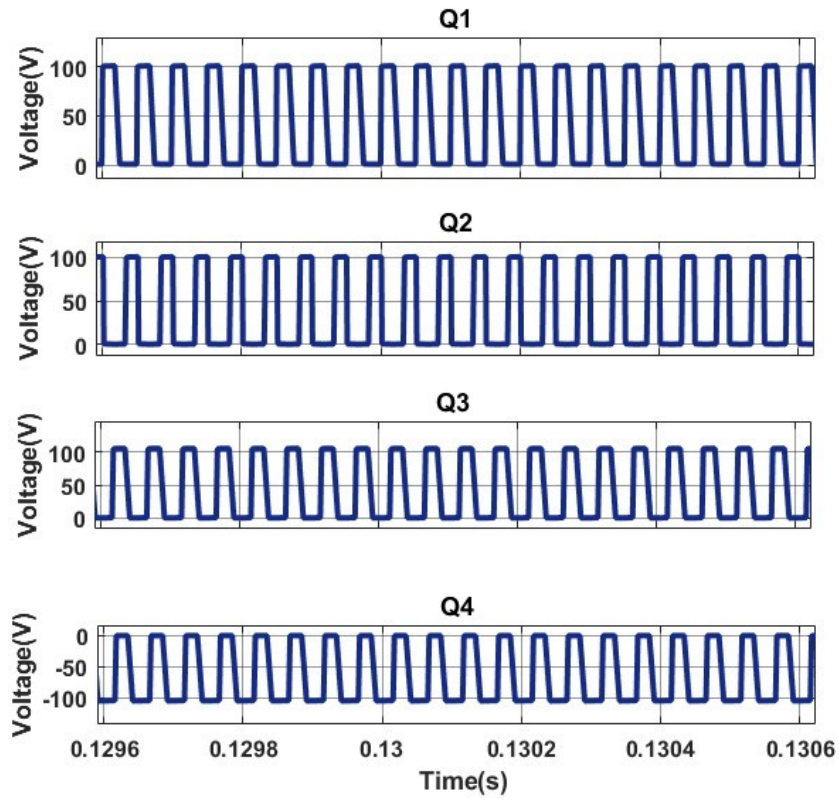


Fig. 5.13: Voltage across switches Q1-Q4

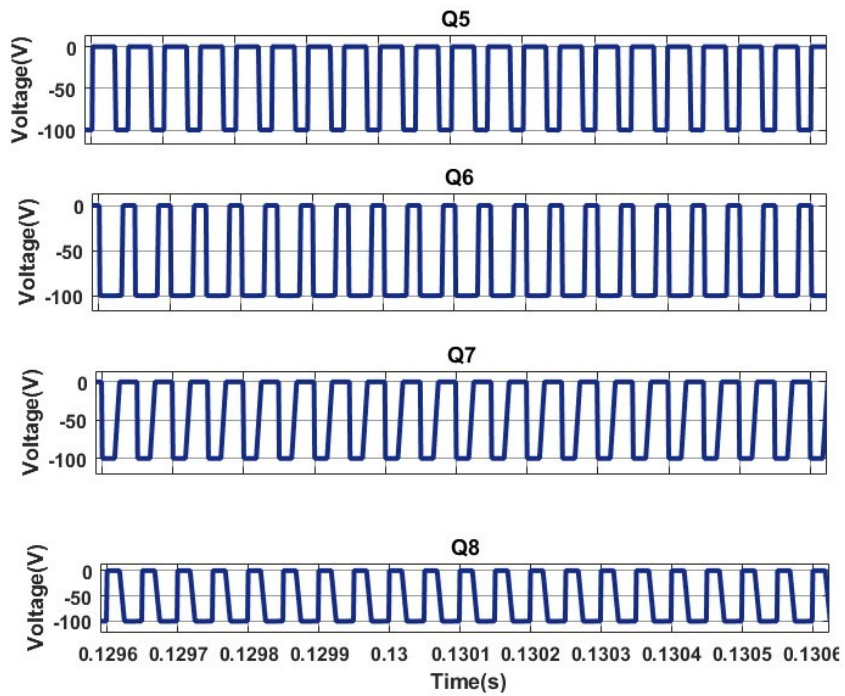


Fig. 5.14: Voltage across switches Q5-Q8

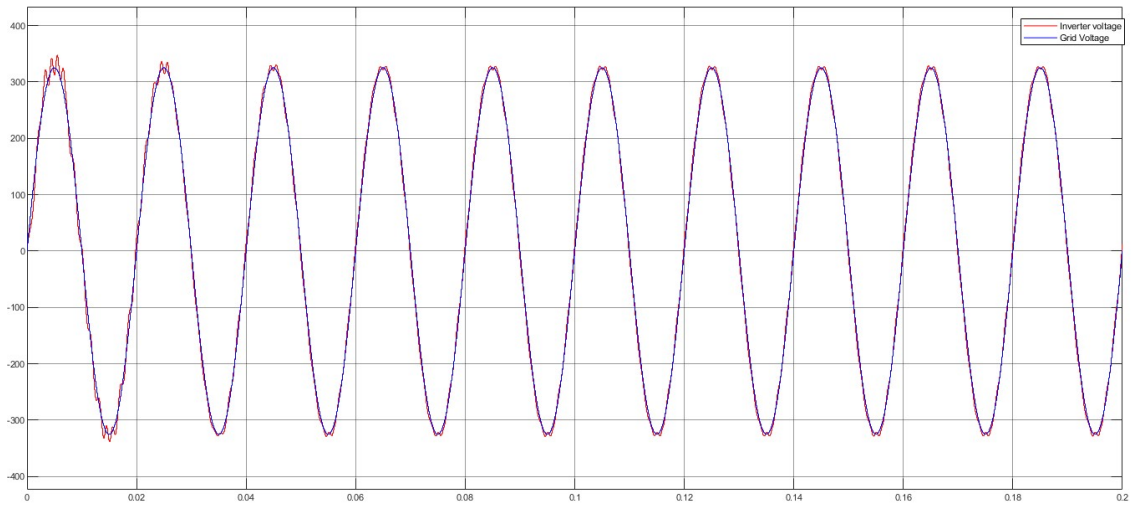


Fig. 5.15: Synchronised AC grid voltage and inverter voltage

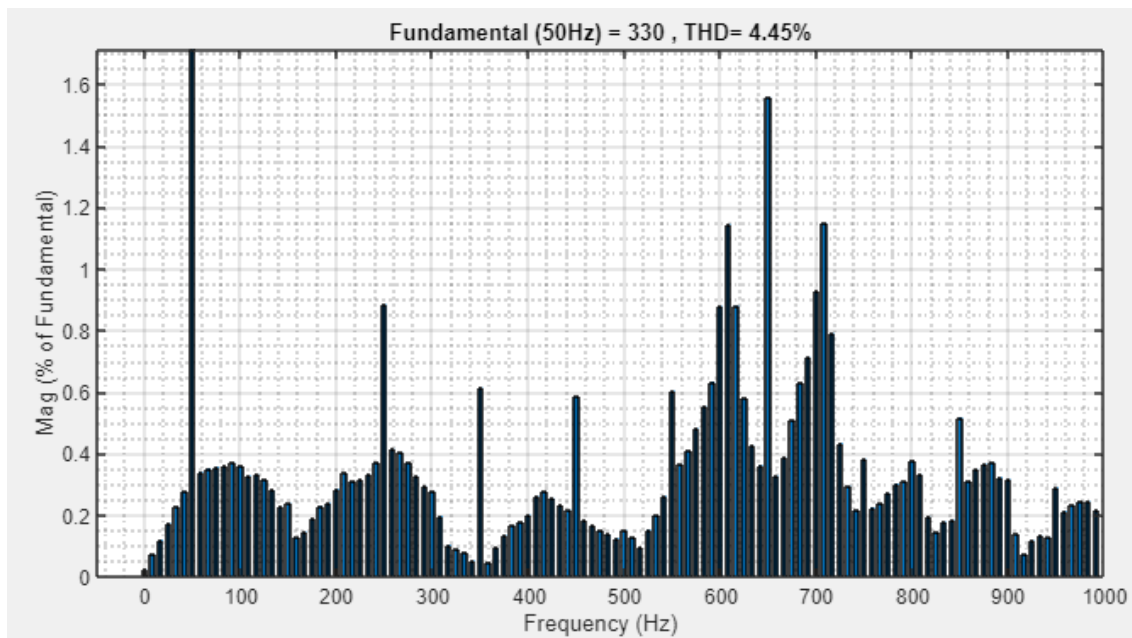


Fig. 5.16: THD Analysis of AC sine wave inverter output

5.4 Conclusion

The output DC voltages and the 230 V, 50 Hz AC voltages are found to be maintained irrespective of the change in irradiance condition. The H bridge inverter voltage and current is also found to be synchronised with the grid voltage and current respectively, while using both the converters.

Table 5.1: Comparison of Converter output quality

Type of Converter	Ripple Factor			THD(%)
	MV DC1	MV DC2	HV DC	230 V, 50 Hz AC
Switched Capacitor Interleaved Bidirectional Converter	0.94	0.89	0.64	4.45
Cascaded Buck Boost Bidirectional converter	1.6	1.2	0.86	5.77

Switched Capacitor Interleaved BDC is discovered to reduce the ripple factors of the output DC buses compared to Cascaded Buck boost BDC. While compared to the earlier conventional converter, the THD (Total Harmonic Distortion) is also lowered with the use of the SCIB converter.

Chapter 6

Conclusion

The PV battery storage based AC-DC hybrid nanogrid system with four different DC voltage buses and an AC bus for supplying AC loads and grid using cascaded buck boost bidirectional converter is designed and simulated in MATLAB. Open loop & closed loop simulation of switched capacitor interleaved bidirectional converter is also simulated. The PV battery storage based AC-DC hybrid nanogrid system with four different DC voltage buses and an AC bus for supplying AC loads and grid using switched capacitor interleaved bidirectional converter is designed and simulated. The performance of the system with cascaded buck boost bidirectional converter and SCIB Converter are studied and compared. The ripples and THD in the system is found to be reduced with SCIB converter and thus efficiency is improved. The voltage stress on switches range from 200 V in the lower converter and above 320 V in the second level cascaded converter in the conventional converter. At the same time, the voltage stress on all the switches in the SCIB converter is found to be approximately one-third of the HV bus voltage. Thus, the voltage stress is also improved with the new converter.

Publications

[1] Amina Shajahan, Baiju R Naina, "An AC – DC Hybrid Nanogrid System with Switched capacitor interleaved bidirectional converter", communicated to International Conference on Power Engineering and Intelligent Systems(PEIS 2023).

Bibliography

- [1] Liangzi Li; Ke-Jun Li; Kaiqi Sun; Zhijie Liu; Wei-Jen Lee, *A Comparative Study on Voltage Level Standard for DC Residential Power Systems*, IEEE Transactions on Industry Applications, Vol. 58, Issue: 2, March-April 2022.
- [2] Subhendu Dutta and Kishore Chatterjee, *An AC-DC hybrid nanogrid system for PV and battery storage based futuristic buildings*, IEEE journal of emerging and selected topics in industrial electronics, vol. 2, no. 3, July 2021.
- [3] Shoaib Rauf, Ali Raza Kalair, and Nasrullah Khan, *Variable Load Demand Scheme for Hybrid AC/DC Nanogrid*, International journal of photoenergy, Hindawi, 2020.
- [4] Kiran Siraj, Hassan Abbas Khan, DC distribution for residential power networks—A framework to analyze the impact of voltage levels on energy efficiency, Energy reports, Elsevier, 2020.
- [5] Yun Zhang, Wei Zhang , Fei Gao , Shenghan Gao, Daniel J. Rogers , *A Switched-Capacitor Interleaved Bidirectional Converter With Wide Voltage-Gain Range for Super Capacitors in EVs*, IEEE Trans. Power electronics, vol. 35, no. 2, February 2020.
- [6] Amber Rasheed; Sidra Khan; Hasan Erteza Gelani; Faizan Dastgeer, *AC vs. DC Home: An Efficiency Comparison*, International Symposium on Recent Advances in Electrical Engineering (RAEE), 2019.

- [7] Y. Xia, W. Wei, M. Yu, X. Wang, and Y. Peng, *Power management for a hybrid AC/DC microgrid with multiple subgrids*, IEEE Trans. Power Electron., vol. 33, no. 4, pp. 3520–3533, Apr. 2018.
- [8] Beiming Liang, Li Kang, Zhaoyun Zhang, Biwu Hu, Yang Zhao, Guozhong Liu, Zhi Zhang, Na Yao, *Simulation Analysis of Grid-connected AC/DC Hybrid Microgrid*, IEEE Conference on Industrial Electronics and Applications, 2018.
- [9] N. Sasidharan and J. G. Singh, *A novel single-stage single-phase reconfigurable inverter topology for a solar powered hybrid AC/DC home*, IEEE Trans. Ind. Electron., vol. 64, no. 4, pp. 2820–2828, Apr. 2017.
- [10] H. Kim, B. Parkhideh, T. D. Bongers, and H. Gao, *Reconfigurable solar converter: A single-stage power conversion PV-battery system*, IEEE Trans. Power Electron., vol. 28, no. 8, pp. 3788–3797, Aug. 2013.
- [11] B. T. Patterson, *DC, Come home: DC microgrids and the birth of the “Ener-net*, IEEE Power Energy Mag., vol. 10, no. 6, pp. 60–69, Nov. 2012.
- [12] <https://mnre.gov.in/solar/current-status/>